ABSTRACT

Title of Thesis: BIODEGRADABLE PRUSSIAN BLUE NANOPARTICLES FOR PHOTOTHERMAL IMMUNOTHERAPY OF ADVANCED CANCERS

Juliana Cano-Mejia, M.S., 2015

Thesis Directed By: Dr. Rohan Fernandes,
Children's National Medical Center,
Washington D.C.

Multifunctional nanoparticles represent a class of materials with diverse therapy and imaging properties that can be exploited for the treatment of cancers that have significantly progressed or advanced, which are associated with a poor patient prognosis. Here, we describe the use of biodegradable Prussian blue nanoparticles (PBNPs) in combination with anti-CTLA-4 checkpoint blockade immunotherapy for the treatment of advanced cancers. Our nanoparticle synthesis scheme yields PBNPs that possess pH-dependent intratumoral stability and photothermal therapy (PTT) properties, and degrade under mildly alkaline conditions mimicking the blood and lymph. Studies using PBNPs for PTT in a mouse model of neuroblastoma, a hard-to-treat cancer, demonstrate that PTT causes rapid reduction of tumor burden and growth rates, but results in incomplete responses to therapy and tumor relapse. Studies to elucidate the underlying immunological responses demonstrate that PTT causes increased tumor infiltration of lymphocytes and T cells and a systemic activation of T cells against re-exposed tumor

cells in a subset of treated mice. PBNP-based PTT in combination with anti-CTLA-4 immunotherapy results in complete tumor regression and long-term survival in 55.5% of neuroblastoma tumor-bearing mice compared to only 12.5% survival in mice treated with anti-CTLA-4 alone and 0% survival both in mice treated with PTT alone, or remaining untreated. Further, all of the combination therapy-treated mice exhibit protection against tumor rechallenge indicating the development of antitumor immunity as a consequence of therapy. Our studies indicate the immense potential of our combination photothermal immunotherapy in improving the prognosis and outlook for patients with advanced cancers.

BIODEGRADABLE PRUSSIAN BLUE NANOPARTICLES FOR PHOTOTHERMAL IMMUNOTHERAPY OF ADVANCED CANCERS

by

Juliana Cano-Mejia

Thesis submitted to the Faculty of the Graduate School of the
University of Maryland, College Park, in partial fulfillment
of the requirements for the degree of
Master of Science
2015

Advisory Committee:
Dr. Rohan Fernandes, Chair
Dr. John P. Fisher
Dr. William Bentley

Dedication

To my parents and brother, for their love, guidance, support, and patience.

Acknowledgements

First and foremost, I would like to thank my advisor Dr. Rohan Fernandes, whose support and guidance made this thesis work possible. He allowed me to pursue my own ideas, and develop research questions that challenged me through all the ups and downs. Without his perseverance, thoughtfulness, and genuine concern, this degree would not have been possible. I could not have asked for a better mentor.

I would also like to acknowledge my committee members: Dr. John Fisher and Dr. William Bentley; for letting my defense be an enjoyable moment, and for their comments and suggestions. I greatly appreciate their contributions, insight, and commitment to further improve this body of work.

Thanks to my lab mates, both past and present: Lizie, Rachel, Shraddha, Erin, Jenny, and Angelina. They have contributed immensely to my personal and professional time at Children's National Health System. I enjoyed their company every day, whether its at our desks, lab, or in the animal room – they all make coming to work an enjoyable moment. Thanks for addressing my questions, helping me with my research, and sharing your experiences with me.

This work would not have been possible without the help and contributions of our collaborators. Dr. Raymond Sze, Dr. Catherine Bollard, and Lina Chakrabarti – Thank you for all your contributions to this work. Thank you to Dr. Conrad Russell Y. Cruz for patiently explaining the immunology concepts of this project and for his insightful comments when designing and planning experiments. Thank you to Dr. Anthony Sandler for sharing his expertise in neuroblastoma biology, and for the practical and straightforward advice he gave for my results.

I gratefully acknowledge the funding sources that made this work possible. My work was supported by the Sheikh Zayed Institute for Pediatric Surgical Innovation at Children's National Health System, and the NSF LSAMP Bridge to the Doctorate Fellowship.

Lastly, I would like to acknowledge the most important people in my life – my family: Mami, Papiro and David for supporting me in everything I do. I cannot thank them enough for loving me and encouraging me throughout this experience. They are my heart and my inner strength.

Table of Contents

List of Tables

List of Figures

Chapter 1: Introduction

1.1 Advanced cancers are a significant health concern

Advanced cancer is a term commonly used to describe primary cancers that are hard to treat, or that have disseminated and formed secondary (metastatic) cancers. These types of cancers are resistant to conventional therapies, and thus there is a significant need for new and innovative treatments to combat these types of cancers. In this thesis, we have chosen neuroblastoma as a representative model of advanced cancers due to their high-risk and difficulty to treat in patients.

1.2 Neuroblastoma as a representative model of advanced cancers

Neuroblastoma is the third most common pediatric cancer and the most common extracranial solid tumor in children accounting for 15% of cancer-related deaths in the pediatric age group[1-2]. More than 50% of neuroblastoma patients present with regional or distant-stage disease at initial diagnosis. Even though progress has been made over the last 20 years in the management and treatment of low-risk and intermediate-risk neuroblastoma patients, the prognosis for patients with high-risk neuroblastoma has remained low.[3] The overall survival rate in this patient population is at 30-40%.[4] Various treatment modalities such as surgery, chemotherapy, radiation therapy, retinoid therapy, and high dose radio/chemotherapy with stem cell transplant have made incremental but limited progress in treating patients with high-risk neuroblastoma.[3] Hence there is an urgent need to develop novel and effective therapies for patients with this resistant and advanced tumor.

1.3 Key challenges in treating high-risk neuroblastomas

Despite being a prevalent tumor, the etiology of neuroblastoma is not well understood. There are no known risk factors and there is no clear genetic predisposition for developing the disease. The efficacy of new candidate drugs on neuroblastoma cell lines does not translate into clinical efficacy because of problems associated with drug penetration and distribution within these tumors. Conventional research in cancer resistance has typically focused on the molecular mechanisms of resistance and has neglected the role of drug penetration and distribution within tumors. Despite improvements in diagnosis and surgical techniques, most deaths from neuroblastoma are due to advanced cancers that have metastasized or are resistant to conventional therapies. Therefore, the next generation cancer therapy should be able to target and remove the advanced primary tumor as well as elicit a response that will aid in the elimination of any remaining, distal, or metastatic tumors.

1.4 Nanoparticles in the treatment of advanced cancers

Recent advances in nanotechnology have facilitated the synthesis of multifunctional nanoparticles that exhibit properties that make them attractive candidates for use in the treatment of neuroblastoma. These properties, not observed in the current therapies for neuroblastoma, include: 1) 10-200 nm size ranges that enable nanoparticles to extravasate into tumors with poorly differentiated vasculature and lack of functional lymphatics via EPR effect,[5-6] 2) High surface area-to-volume ratios for biofunctionalizing the nanoparticles for long circulation, or for attaching ligands that target receptors overexpressed on tumor cells,[7-9] and 3) The ability to carry or be used themselves as

therapeutic agents at the tumor sites (e.g. photothermal therapies and photothermal immunotherapies).[9]

1.5 Photothermal immunotherapy of advanced cancers

As mentioned before, advanced cancers such as neuroblastoma are more efficiently treated with combination treatments that aim at not only debulking the primary tumor, but also initiating an anti-tumor response. In response to this need for more effective therapies for neuroblastoma, we developed a combination therapy termed photothermal immunotherapy, which synergistically combines two treatments: 1) nanoparticle-based photothermal therapy, which provides a minimally invasive method to shrink primary tumors while simultaneously providing a robust vaccination effect by breaking up the cancer and releasing its antigens, and 2) checkpoint blockade immunotherapy, which reverses the suppressive effects of these tumors on the immune system, and unleashes a potent, systemic antitumor immune response. Success in these studies will facilitate our long-term goal of advancing this novel combination therapy to the clinic to treat patients with high-risk neuroblastoma, offering the potential for an improved prognosis for this patient population.

1.6 Prussian blue nanoparticles for photothermal therapy of cancers

Photothermal therapy (PTT) using Prussian blue nanoparticles (PBNPs) is a minimally invasive, *in situ* method for ablating cancer cells and reducing tumor burden.[10] In this treatment modality, NIR light-absorbing PBNPs are injected into tumors and irradiated with a low-power NIR laser, resulting in rapid heating of the nanoparticles and destruction of the tumor. Therefore, PTT can serve as an alternative to surgery, which is one of the standards of care for neuroblastoma. As compared to other nanoparticles that

have been used for PTT, we have the ability to synthesize PBNPs that safely biodegrade in physiological media, thus mitigating concerns associated with the long-term fate and toxicity of nanoparticles within the body. Further, PBNPs can be easily synthesized in a scalable manner in a single-step at low costs,[10-13] and is already FDA-approved for human oral use (to treat radioactive poisoning).[14-16]

As a therapeutic platform, PBNP-based PTT offers enormous flexibility compared to other hyperthermia and thermal ablation methods (e.g. HIFU, RF ablation, cryoablation)[17-19] that have been used for tumor therapy and are being investigated in combination with immunotherapies. Our Prussian blue nanoparticles can be easily modified for multiple functions (e.g. they can carry additional immunomodulatory[20-22] or therapeutic molecules),[23-24] an advantage not offered by alternative hyperthermia or thermal ablation methods.

1.7 anti-CLTA-4 for checkpoint blockade immunotherapy

In checkpoint blockade immunotherapy, monoclonal antibodies (mAbs) targeting checkpoint inhibitors decrease immunosuppression and elicit a potent immune response. Various mAbs targeting checkpoint inhibitors (e.g. nivolumab: anti-PD-1 and ipilimumab: anti-CTLA-4)[25] are now in clinical trials and have received approval for treatment of cancers (e.g. ipilimumab for metastatic melanoma)[26]. Despite this progress, the vast majority of tumor antigens that function as targets of T cells activated by checkpoint blockade immunotherapy remain to be identified[27-28]. Further, it is not known whether these antigens can be used to generate tumor-specific vaccines for an enhanced therapeutic effect. Recent preclinical studies have utilized nucleic acid or peptide vaccines against common neuroblastoma markers in conjunction with checkpoint

blockade immunotherapy,[29-30] this approach requires *a priori* knowledge of the tumor antigens to generate the relevant vaccines. By contrast, our strategy relies on PTT to release tumor antigens to the surrounding milieu,[20, 31-32] and has the potential for increasing tumor immunogenicity via a "multi-antigen vaccination effect" without the need for prior knowledge of the tumor antigens. Hence, PTT in conjunction with checkpoint blockade immunotherapy could fill a major gap in efforts to exploit the immune system against disseminated neuroblastoma.

1.8 Thesis outline and specific aims

Aim 1. Determine the degradation, stability and cytotoxicity of Prussian blue nanoparticles in tumor and physiological environments. We want to control the degradation of Prussian blue nanoparticles so that they can be stable in tumor environments, and degrade in physiological environments. Furthermore, the degradation products will be studied for their cytotoxicity when co-cultured with cells. These studies are important for addressing concerns associated with the long-term fate and associated toxicities of the nanoparticles within the body.

Aim 2. Determine the photothermal therapy capabilities of Prussian blue nanoparticles in a tumor environment. Photothermal heating in tumor and physiological pHs will be determined at various concentrations of Prussian blue nanoparticles to ensure that their photothermal characteristics are maintained in tumor environments.

Aim 3. Determine the efficacy of Prussian blue nanoparticle-based photothermal therapy for treating aggressive cancers. A syngeneic mouse model of neuroblastoma will be used to study the effects that Prussian-blue nanoparticle-based photothermal therapy has on tumor regression.

Aim 4. Determine the effect of Prussian blue nanoparticle-based PTT on stimulating a T cell-mediated response. The goal of this aim is to study the effects of PTT by characterizing the resultant antitumor T cell responses in the mouse model of neuroblastoma. These studies will provide rationale for exploring PTT in combination with anti-CTLA-4

Aim 5. Determine the effect of the combination photothermal immunotherapy on tumor regression and long-term survival in a mouse model of neuroblastoma. We will assess the efficacy of PTT in combination with anti-CTLA-4 in effecting tumor regression and conferring long-term survival in a mouse model of neuroblastoma.

Aim 6. Determine the effect of tumor rechallenge on long-term surviving mice that were previously treated with photothermal immunotherapy. We want to examine if PTT in combination with anti-CTLA-4 confers long-term survival in mice. Mice will be re-challenged with Neuro2a cells, and their tumor progression or regression will be monitored.

Chapter 2: Biodegradable Prussian blue nanoparticles for photothermal immunotherapy of advanced cancers

2.1 Introduction

Recent advances in the field of nanomedicine have yielded diverse nanoparticle-based platforms with multifunctional therapy and imaging ("theranostic") capabilities for human health. An exciting area within this field of research is the application of multifunctional nanoparticles for treating cancer, where numerous nanoparticles have received FDA approval or are currently undergoing clinical evaluation.[33-34] Despite this promise, a key challenge confronting the field is developing therapies for cancers that have significantly progressed or metastasized, i.e. advanced cancers, for which the prognosis is dismal (e.g. the five-year survival rate is 40%-50% for patients with high-risk neuroblastoma[1, 3] and 16.6% for patients with metastatic melanoma).[35] In response to this need, we are exploring a novel combination therapy termed photothermal immunotherapy, which combines Prussian blue nanoparticle (PBNP)-based photothermal therapy (PTT) with checkpoint blockade immunotherapy for treating advanced cancers.

In nanoparticle-based PTT, near infrared (NIR) light-absorbing nanoparticles accumulate within tumors after either intratumoral or intravenous injection, and heat up when illuminated with a low power (< 2 W) NIR laser, causing destruction of tumor cells.[36-37] The heating effect is negligible when the low power laser is used without the nanoparticles, since human tissue exhibits a "window" of decreased light absorption at NIR wavelengths.[38-39] Thus, PTT functions as a rapid and minimally invasive method for reducing tumor burden. Several reports have demonstrated the efficacy of diverse nanoparticles including gold nanoshells,[40-41] gold nanorods,[36, 42] gold nanocages,[43-44] and

carbon nanotubes[45-46] in reducing tumor growth rates and, in some cases, conferring long-term, tumor-free survival in animal models (e.g. breast cancer,[47] squamous cell carcinoma,[48] prostate cancer[49]). Despite this promise PTT alone is generally ineffective in treating advanced cancers[10, 31-32] and the dual requirement for nanoparticles and an activating laser to secure a therapeutic effect argues against the use of PTT alone for treating advanced disease. We propose that besides local tumor damage, PTT may release tumor antigens that could be exploited for immunotherapy. We thus hypothesized that combining PTT with checkpoint blockade immunotherapy would allow for T-cell expansion and induce immune mediated tumor cell killing even in advanced cancers.

Checkpoint blockade uses monoclonal antibodies to target key immune checkpoints such as CTLA-4 and PD-1[50] in order to reverse immune suppression, unleashing potent antitumor responses by activating endogenous immune cells (e.g. T cells).[51-52] Checkpoint inhibitors including anti-CTLA-4 (e.g. ipilimumab) and anti-PD-1 (e.g. nivolumab) have received FDA approval for the treatment of advanced cancers such as metastatic melanoma.[25-26] Still, the responses in advanced cancers treated with checkpoint inhibitors are restricted to only a modest subset of patients. For example, in a recent study, only 22% of patients with metastatic melanoma treated with both anti-CTLA-4 and anti-PD-1 exhibited a complete response to treatment.[53] This restricted response may be attributed to the fact that checkpoint inhibitors result in blanket activation of endogenous immune cells and are not delivered in the context of antigen processing necessary for tumor-specific effects. Another limitation of using checkpoint inhibitors alone is that at high doses they are associated with toxicity and potentially lethal non-specific immune-mediated adverse events due to hyper-immune activation.[53]

An intriguing strategy for simultaneously improving the efficacy of checkpoint inhibitors and decreasing their toxicity lies in providing immune cells reactivated by checkpoint inhibitors with an abundance of the appropriate tumor-specific antigen targets. To this end, various vaccines have been combined with checkpoint inhibitors and have shown promise in preclinical and clinical studies.[29-30, 54-55] However, all of these approaches require *a priori* knowledge of the tumor antigens or manipulated tumor cells to generate the relevant vaccines. The problem is compounded by the highly heterogeneous nature and dynamic phenotypic and metabolic landscape of advanced cancers, which have impeded efforts to identify valid antigen-expression profiles for vaccine development.

In this paper, we present an alternative approach where we locally ablate tumors at their sites of localization using nanoparticle-based PTT, thus generating an "*in situ*" vaccine by disrupting the tumor mass and enhancing its immunogenicity by exposing potential tumor antigens. Specifically, our combination therapy (**Fig. 1**) uses 1) biodegradable PBNPs for PTT where PBNPs are administered intratumorally and irradiated with an NIR laser, serving the dual purpose of primary tumor ablation and *in situ* vaccination, and 2) anti-CTLA-4 checkpoint blockade immunotherapy by intraperitoneal (i.p.) administration, that causes expansion of cytotoxic immune effector T cells that are the key to providing a robust antitumor immune response. As proof-of-concept, we tested the efficacy of this combination therapy termed photothermal immunotherapy in a mouse model of advanced neuroblastoma.[52, 56-57] We hypothesized that the novel combination of two therapies – PBNP-based PTT and anti-CTLA-4 checkpoint blockade immunotherapy – will act synergistically to improve outcome over those obtained with either modality alone.

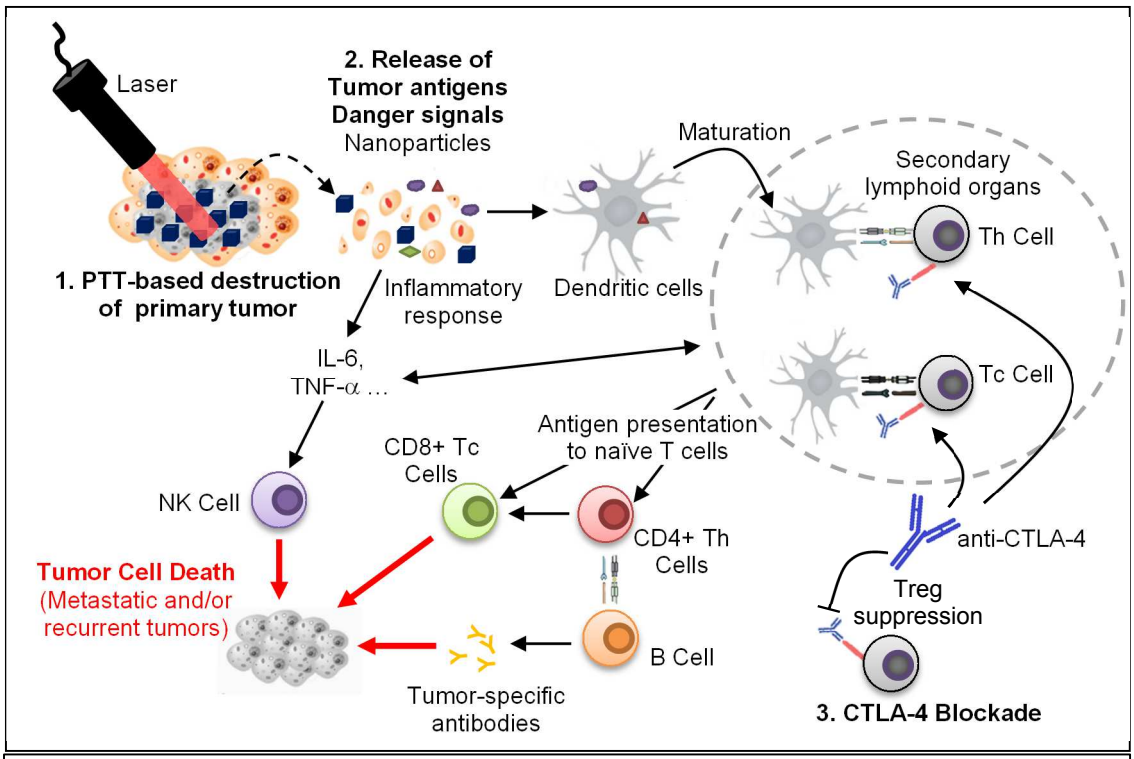

Figure 1. Hypothesized mechanism of action of photothermal immunotherapy. The novelty of our combination photothermal immunotherapy includes: 1) PTT-based destruction of tumors in a minimally invasive manner, 2) Release of tumor antigens and danger signals post-PTT providing an immunostimulatory, multi-antigen vaccination effect, and the 3) Use of anti-CTLA-4 that reverses immunosuppression and unleashes a potent antitumor immune response. A hypothesized mechanism of action of the combination photothermal immunotherapy using Prussian blue nanoparticle-based PTT and anti-CTLA-4 checkpoint blockade immunotherapy is presented. PTT ablates the PTT ablates the primary tumor, providing tumor antigens and danger signals that activate dendritic cells. These antigens released by dying cells are captured by dendritic cells, processed into peptides and presented to CD4+Th cells. Once activated, effector T cells may help generate an immune response through the activation of cytotoxic CD8+T cells that can eradicate tumors. Additionally, tumor-infiltrating B cells may also help present tumor-associated antigens for the induction of a CD4+Th cell-mediated cellular immunity. Furthermore, CTLA-4 blockade results in direct activation of CD4+ and CD8+ effector T cells, resulting in an antitumor T cell response. The combinations of some or all of these immune responses result in the elimination of the primary tumor as well as metastatic/recurrent tumors

As compared with other ablative and tumor disruptive techniques such as radiofrequency ablation[58-59], high-intensity focused ultrasound,[60] and cryoablation[61] that can be combined with checkpoint inhibitors to treat aggressive cancers, nanoparticle-based PTT offers enormous flexibility. The nanoparticles can be modified for multiple functions (e.g. they can carry additional immunomodulatory[20-22] or therapeutic molecules),[23-24] an advantage not offered by the aforementioned alternative techniques. As compared to other

nanoparticles used for PTT, including a promising recent report by Wang *et al.*[32] describing carbon nanotube-based PTT in combination anti-CTLA-4 in a mouse model of breast cancer, our PBNPs offer advantages in that they are non-toxic, easily synthesized in a single step,[10-13] and are already US FDA-approved for human oral consumption (to treat radioactive poisoning).[14-16] Importantly, PBNPs are biodegradable thus mitigating concerns associated with the long-term fate and associated toxicities of using nanoparticles *in vivo*.

Herein, we characterize the biodegradation of PBNPs by testing temporal stability at various pHs levels (mimicking conditions observed in the tumor interstitium, lymph, and blood). Next, we measure the ability of the biodegradable PBNPs to be used for PTT and the effect of the PTT on tumor growth rates relative to untreated controls in the mouse model of neuroblastoma. We also measure the ability of the PTT to elicit a tumor-specific T cell response and determined the effect of our combination therapy (PTT + anti-CTLA-4) on tumor growth rates and survival in the neuroblastoma mouse model relative to mice treated with either therapy (PTT or anti-CTLA-4) alone or remaining untreated. Finally, we evaluate long-term tumor immunity in mice cured of their disease.

2.2 Methods

2.2.1 Materials

All synthetic procedures were conducted using ultrapure water obtained from a Milli-Q system (Millipore Corporation, Billerica, MA) with resistivity of 18.2 M Ω ·cm. Potassium hexacyanoferrate (II) trihydrate (MW 422.39; $K_4[Fe(CN)_6]\cdot 3H_2O$) and iron

(III) chloride hexahydrate (MW 270.3; $Fe(Cl)_3 \cdot 6H_2O$) were purchased from Sigma-Aldrich (St. Louis, MO).

2.2.2 Antibodies and cells

Anti-CTLA-4 antibody (9D9) was purchased from BioXCell (West Lebanon, NH). Mouse CD45-FITC and CD3-FITC antibodies were purchased from eBioscience (San Diego, CA). The murine neuroblastoma cell line Neuro2a was originally obtained from American Type Culture Collections (ATCC) and cultured under recommended conditions. Cells were cultured in DMEM (Gibco, Carlsbad, CA) containing 10% fetal bovine serum (FBS, Gibco, Carlsbad, CA) and 1% penicillin/streptomycin (Sigma-Aldrich, St. Louis, MO). Luciferase-expressing Neuro2a cells were constructed by transducing the Neuro2a cells with firefly luciferase-expressing lentiviral particles (GenTarget Inc., San Diego, CA) and selecting with puromycin (Thermo Fisher, Waltham, MA). Luciferase expression was determined by measuring bioluminescence in a luminometer using the Luciferase Assay System (Promega, Madison, WI).

2.2.3 Animals

Four-to-six-week old female A/J mice were purchased from Jackson Laboratory (Bar Harbor, ME). The animals were acclimated for 3-4 days prior to tumor inoculation. All procedures were approved by the Institutional Animal Care and Use Committee of Children's National Health System, Washington, DC (Protocol # 00030439).

2.2.4 Prussian blue nanoparticles synthesis

Prussian blue nanoparticles were synthesized using a scheme as described previously.[10] Briefly, an aqueous solution of 6.8 mg $FeCl_3 \cdot 6H_2O$ (2.5×10^{-5} mol) in 5 mL of Milli-Q water was added under vigorous stirring to an aqueous solution containing 10.6 mg of

$K_4Fe(CN)_6 \cdot 3H_2O$ (2.5×10^{-5} mol) in 5 mL of Milli-Q water. After stirring for 15 min, the precipitate was isolated by centrifugation (20,000 xg for 5 min) and rinsed by sonication (5 s, high power) in Milli-Q water. The isolation and rinsing steps were repeated three times before the particles were resuspended by sonication in Milli-Q water.

2.2.5 Prussian blue nanoparticles stability and degradation studies

The sizes and zeta potentials of all particles were measured using a Zetasizer Nano ZS (Malvern Instruments, Worcestershire, U.K.). PBNP suspensions were resuspended in pH 7.4 or pH 5.5. These solutions were made using appropriate amounts of mild acids and bases to Milli-Q water until the desired pHs were obtained. Analyses were then performed using the manufacturer's specifications. The Vis-NIR absorbance spectra of the nanoparticles in the varied pHs were measured using the VISIONlite software on the Genesys 10S spectrophotometer (Thermo Scientific, Waltham, MA).

2.2.6 Prussian blue nanoparticles cytotoxicity studies

PBNPs (0.03 mg/mL) were suspended in pH 7.0 or 7.4 solution, and their degradation products were co-incubated with Neuro2a cells *in vitro*. Cell viability after incubation with the degradation products was measured using the XTT assay (Trevigen, Gaithersburg, MD) as per manufacturer's protocol where the absorbance of metabolized product indicates viability.

2.2.7 In vitro photothermal therapy

PTT *in vitro* was performed using an 808 nm NIR laser from Laserglow Technologies (Toronto, ON, Canada) at a power of 1.875 W/cm^2. PBNPs at concentrations of 0.01 mg/mL, 0.1 mg/mL, and 1 mg/mL were resuspended in a pH of 7.4 or 5.5, plated in a 96-

well plate, and irradiated for ten minutes. Temporal temperature measurements were taken using a thermocouple (Omega, Stamford, CT).

2.2.8 Establishment of a mouse neuroblastoma model

For establishing primary tumors and for the rechallenge studies, 10^6 Neuro2a cells transfected with luciferase were suspended in PBS and subcutaneously injected into the back of each previously shaved mouse. Tumor growth was monitored on alternate days following tumor inoculation by imaging the mice for tumor bioluminescence using the IVIS Lumina III (PerkinElmer). This animal imaging system allows for quantitative analysis of tumor volume over time. Tumor volumes were calculated using this imaging system as previously described.[62] A tumor size of 17 mm diameter in any dimension was designated as the endpoint and mice were euthanized at that time. Euthanasia was achieved through cervical dislocation after CO_2 narcosis. If the tumor impaired mobility of the animal, became ulcerated or appeared infected, or if the mice displayed signs of distress by sick mouse posture, the mice were euthanized and removed from the group.

2.2.9 In vivo photothermal therapy

For photothermal therapy (PTT) *in vivo*, neuroblastoma-bearing mice were treated when their tumor volumes reached ~60mm^3. Mice were anesthetized prior to and during treatment using 2-5% isoflurane. The mice were intratumorally injected with 50 μL of PBNPs (1 mg/mL), and the tumor area was irradiated with an 808 nm NIR laser (Laserglow Technologies; Toronto, ON, Canada) at 1.875 W/cm^2 for 10 minutes. The animals' eyes were covered with opaque black cardboard during treatment to avoid eye damage by the laser. The temperatures reached during PTT were measured using a FLIR thermal camera (Arlington, VA).

2.2.10 Anti-CLTA-4 injections

Anti-CTLA-4 antibody (150 μg per mouse) was administered intra-peritoneally (i.p.) on days 1, 4, and 7 for the combination (PTT + aCTLA-4) group, and on days 0, 3, and 7 for the anti-CTLA-4 only group.

2.2.11 T cell mediated response studies

Whole tumors were extracted from experimental and control tumor-bearing mice, and were minced and run through a 70μm filter. Once single cell suspensions were obtained, the tumor cells were cultured in complete DMEM medium prior to studies. Tumor isolate was used to assess leukocyte infiltrate by flow cytometry. Cells were stained with CD45 and CD3 antibodies conjugated to FITC (BD Biosciences) and samples were run on the BD Accuri cytometer at a threshold of 80,000. Analysis of flow cytometry results was conducted in FlowJo 7.6 (TreeStar Inc.) and populations of interest and mean fluorescence intensity (MFI) were determined from ungated live samples.

2.2.12 IFN-γ expression studies

T cells were harvested from spleens of tumor-bearing mice and isolated with CD5 immunomagnetic beads (Ly-1, Miltenyi Biotec). 200,000 murine T cells were included in an ELISpot assay (IFN-γ ELISpot, Mabtech, Inc.) at 1:1 with *ex vivo* tumor cells, which was conducted according to the manufacturer's protocol. Splenocytes and isolated T cells were cultured in complete RPMI medium.

2.2.13 Statistical analysis

Statistical significance between groups was determined using a Student's *t*-test. Significant difference between two groups of flow cytometry data was determined using a chi-square test. To determine minimum sample sizes for each group in the animal

studies, we conducted a power analysis using α = 0.05 (Type I error probability associated with this test of this null hypothesis) and power = 0.8. After inputting the values of σ / δ for each t-test (using PS power and sample size software), we calculated the number of mice/group needed to generate statistically meaningful results. Our sample sizes are consistent with those in similar studies published in the literature.[30, 52] The log rank test was used to determine statistically significant differences in survival between the various groups, (α = 0.05, rejecting the null hypothesis of no difference in survival between independent groups if χ^2 exceeds the critical value for the test). Survival results were analyzed according to a Kaplan-Meier curve. A p-value < 0.05 was considered statistically significant.

2.3 Results

2.3.1 Degradation, stability, and cytotoxicity of Prussian blue nanoparticles.

We utilize intratumoral administration of PBNPs for PTT in these studies to maximize nanoparticle dose at the site of injection within the tumor, although this technique could result in poor nanoparticle distribution within the tumor.[63] However, given the nature of our combination therapy where PBNP-based PTT provides a local effect complemented by a systemic effect of anti-CTLA-4 immunotherapy, we posit that the effect of the potentially poor spatial distribution of the nanoparticles would be negligible or overcome by the systemic immunotherapy effect. To assess the suitability of using PBNPs for intratumoral PTT, we conducted studies analyzing the biodegradation, stability, and cytotoxicity of the PBNPs (and potential degradation products) *in vitro*. We measured the degradation and stability of PBNPs using visible-NIR (Vis-NIR) spectroscopy and

dynamic light scattering (DLS) as a function of time and at various pH levels (**Fig. 2**) - mimicking conditions typically encountered by intratumorally administered nanoparticles, i.e. the tumor interstitium, lymphatics, and vasculature. Tumor interstitia exhibit a slightly acidic pH (~5.5),[64-65] while blood and lymph exhibit mildly alkaline pHs (~7.4). We measured the Vis-NIR and DLS properties of PBNPs over seven days at three pHs - 5.5 representing tumor interstitia, 7.0 representing neutral pH, and 7.4 representing blood/lymph.

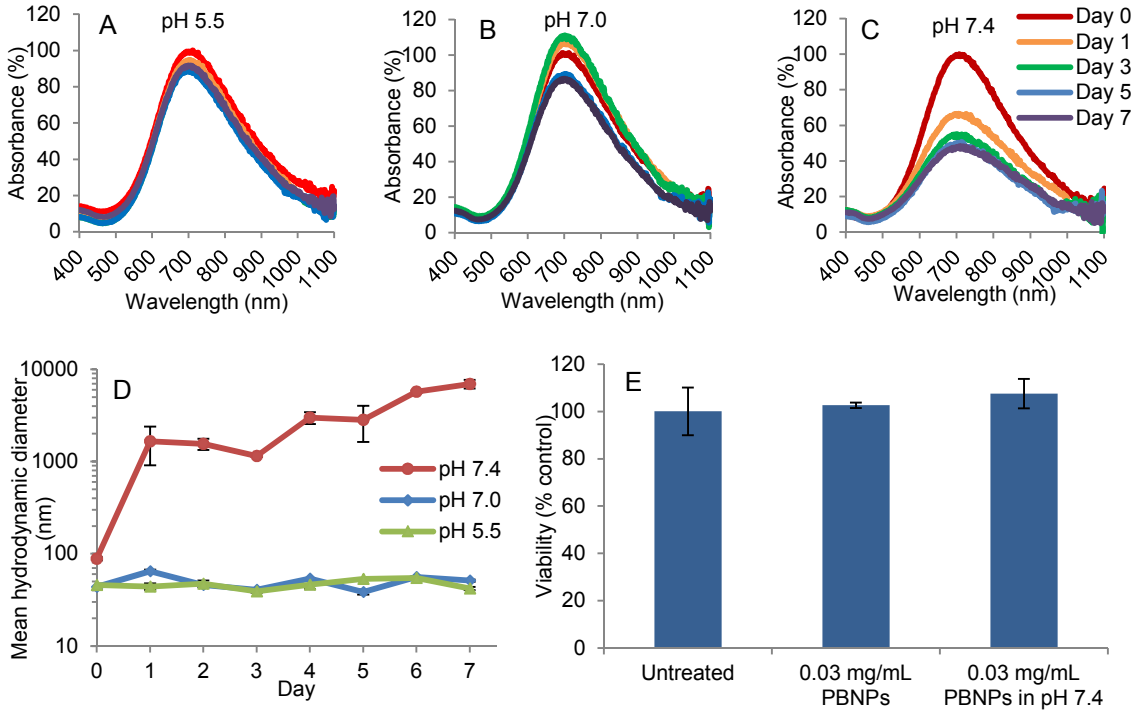

Figure 2. Degradation, stability, and cytotoxicity of PBNPs. (A-C) Degradation properties were quantified by measuring the visible-NIR spectra of PBNPs over seven days (Day 0-7) at A) pH 5.5, B) pH 7.0, and C) pH 7.4, exhibiting increased stability at mildly acidic and neutral pHs (5.5 and 7.0) mimicking pHs observed in tumor interstitia and decreased stability at mildly alkaline pH (7.4) mimicking pH observed in the lymph and blood. D) Stability was quantified by measuring the hydrodynamic diameters (sizes) of PBNPs over seven days at varying pHs (5.5, 7.0, and 7.4) exhibiting increased degradation of PBNPs at mildly alkaline pH. E) Cytotoxicity of the degradation products of PBNPs co-incubated with neuroblastoma (Neuro2a) cells showing insignificant changes in viability when treated with both intact and degraded PBNPs relative to untreated controls. Means ± standard deviation; n=3.

The Vis-NIR spectrum of PBNPs demonstrated its characteristic absorption band from 650-900 nm, corresponding to the energy of the metal-to-metal charge transfer between Fe^{II} and Fe^{III} through the cyanide bridge of the PBNP lattice (λ_{max} = 705 nm) (**Fig. S1**).[10, 12, 66] PBNPs incubated at pH 5.5 (tumor interstitial pH) exhibited negligible change in their Vis-NIR spectra over seven days (**Fig. 2A**) indicating that the PBNPs were insignificantly degraded at pH 5.5 over the seven days. Similarly, insignificant degradation properties were observed with PBNPs incubated at pH 7.0 (**Fig. 2B**). However as the pH of the solution was marginally increased from 7.0 (neutral) to 7.4 (mildly alkaline, mimicking blood and lymph pH), we observed a significant (51%) reduction in their Vis-NIR spectrum peak intensity over the course of seven days (**Fig. 2C**), indicating degradation of the PBNPs at pH 7.4. This was most likely caused by attack of the characteristic Fe^{II}-CN-Fe^{III} bonds of PBNP by the slight excess of hydroxyl ions, as previously observed.[67-68] These observations were corroborated by a temporal DLS study, which was used to assess nanoparticle size distributions and stability, where PBNPs were observed to be stable when incubated at pH 5.5 and 7.0 (constant mean hydrodynamic diameters; **Fig. 2D and S2**). In contrast, DLS demonstrated an increase in the mean hydrodynamic diameter of the PBNPs at pH 7.4 compared to pH 5.5 (**Fig. 2D and S2**), indicating instability and aggregation of the nanoparticles at this blood/lymph-mimicking pH.

We then assessed the cytotoxicity of both the PBNPs and their degradation products on neuroblastoma tumor cells (Neuro2a cells) *in vitro*. For these studies, we incubated 0.03 mg/mL PBNPs or 0.03 mg/mL PBNPs pre-contacted at pH 7.4 (to degrade them) with Neuro2a cells and measured the resultant cell viability using an XTT cell viability assay

(**Fig. 2E**). The concentration of the nanoparticles used in this study was representative of the effective concentrations of the nanoparticles attained after intratumoral administration. We observed that neither the PBNPs nor their degraded products were cytotoxic to Neuro2a cells at these concentrations, i.e. the measured viability was not significantly different from untreated controls (**Fig. 2E**), indicating the suitability of using the PBNPs *in vivo*. Taken together, our findings indicate that our PBNPs are suitable for intratumoral administration as they exhibit an inherent pH-dependent degradation and stability, where they are stable under conditions mimicking the tumor interstitium (lower pH), and degrade and are unstable under conditions mimicking the blood and lymph. Importantly, our findings suggest that the resulting degradation products are not cytotoxic.

2.3.2 Photothermal therapy capabilities of Prussian blue nanoparticles

We conducted studies to determine whether the pH-dependent stability of PBNPs had an effect on their function as PTT agents by assessing their PTT capabilities *in vitro* (**Fig. 3A**) and *in vivo* (**Fig. 3B**). We measured the PTT capabilities of the PBNPs as a function of concentration (0.01 – 1 mg/mL) at the two pHs – 5.5 (representing the tumor interstitial pH at which the nanoparticles are stable) and 7.4 (representing the pH of blood/lymph at which the nanoparticles are unstable). As expected, we observed that the PBNPs heated to higher temperatures when they were incubated in a pH of 5.5 versus 7.4, and this occurred in a concentration-dependent manner (**Fig. 3A**). This is likely due to the fact that at higher pH, PBNPs exhibit a significant reduction in their PTT capabilities due to their degradation and instability under these conditions, consistent with our earlier findings. The reduction in the PTT capabilities was also concentration-

dependent; 1 mg/mL PBNPs incubated at pH 7.4 exhibited a ~16 °C decrease in temperature after PTT compared 1 mg/mL PBNPs at pH 5.5, and 0.1 mg/mL PBNPs exhibited a ~7°C decrease in PTT capabilities between these pHs. Although not studied here, the duration of incubation (hours-days) would also be expected to play a role in the PTT capabilities of the PBNPs as longer incubations under destabilizing conditions (i.e. higher pH) would be expected to further decrease the PTT capabilities of the nanoparticles.

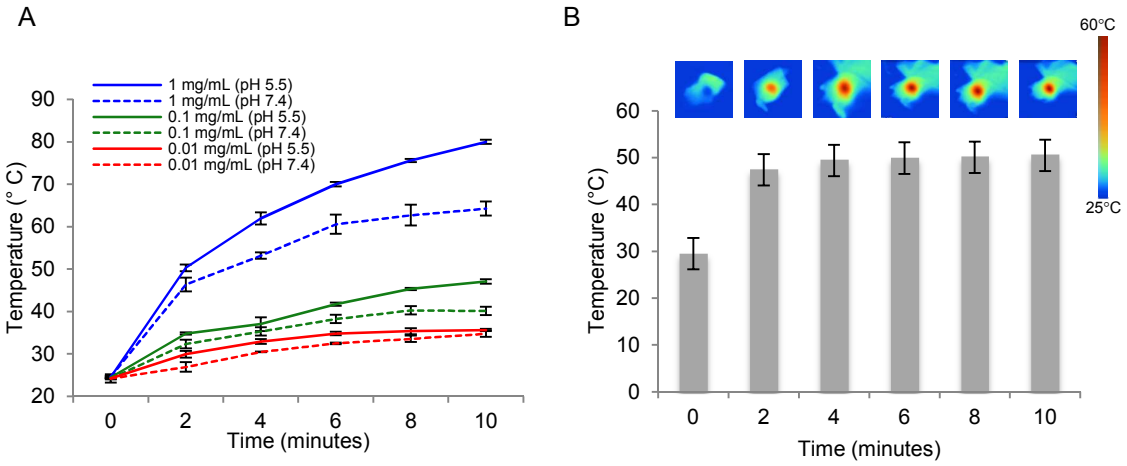

Figure 3. I*n vitro* and *in vivo* PTT capabilities of PBNPs. A) *In vitro* PTT capabilities of varying concentrations of PBNPs at pH 5.5 and 7.4 showing decreased heating at higher pHs. B) Temperatures achieved by intratumorally injected 50 µL (1 mg/mL) PBNPs irradiated with an 808nm NIR laser for 10 minutes at 1.875 W/cm^2. Inset: heat maps showing increased temperatures (~50-55 °C) achieved at the injection site that rapidly decreases to body temperature (~25-30 °C) outside the tumor region.

We then measured the PTT capabilities of the PBNPs in the syngeneic mouse model of neuroblastoma. Given the degradation and stability properties of the PBNPs, the goal of this study was to determine the effective intratumoral dose of the PBNPs to achieve temperatures suitable for thermal ablation of the tumors (i.e. 50-55 °C). Using IR thermography, we determined that mice bearing 5 mm tumors (~60 mm^3 tumor volumes)

intratumorally injected with 50 µL of 1 mg/mL PBNPs were able to heat up to ablative temperatures in 2-4 minutes when irradiated with an 808 nm NIR laser at 1.875 W/cm^2 laser power densities (**Fig. 3B**). The temperature achieved is a function of PBNP dose (concentration and volume) and tumor pH/vasculature/lymphatics. These results indicate that the PBNPs exhibit pH-dependent PTT capabilities where they heat to higher temperatures at intratumoral pH when compared to that of blood and lymph.

2.3.3 Prussian blue nanoparticle-based photothermal therapy for treating aggressive cancers.

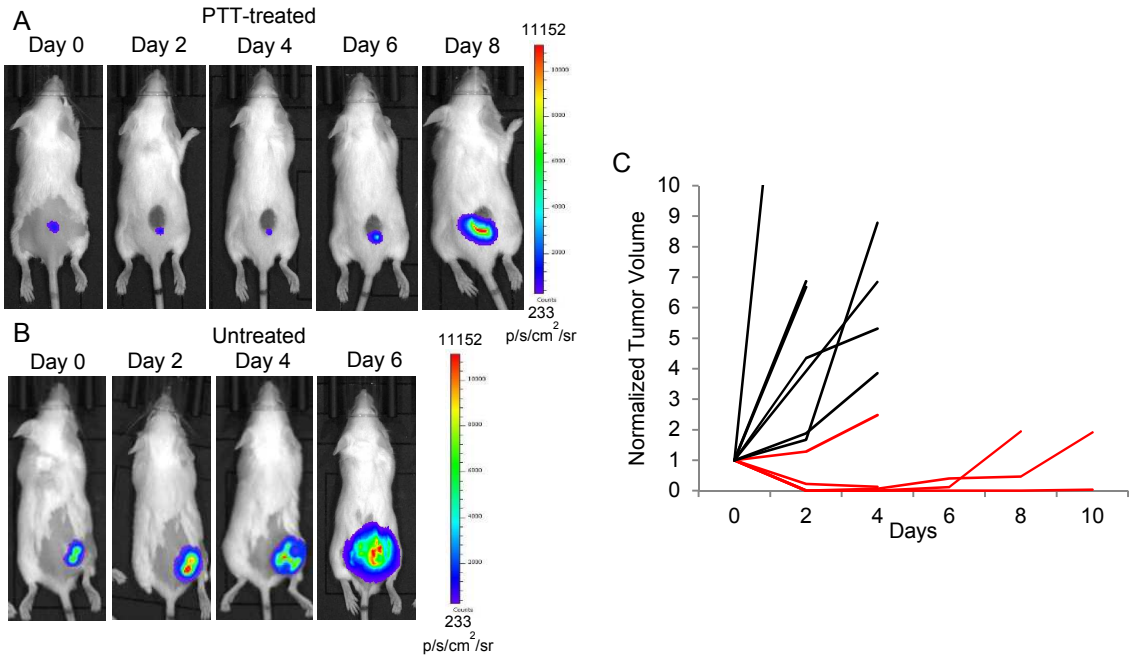

Figure 4. Tumor debulking after PBNP-based PTT *in vivo*. Representative images of A) a PTT-treated mouse showing near complete debulking of the tumor mass after PTT (no measured bioluminescence) and B) an untreated mouse showing faster tumor progression. Scale bars on the right of panels A and B represent the bioluminescent intensity in p/s/cm^2/sr. C) Normalized tumor growth curves for PTT-treated (red; n = 5) and untreated mice (black; n = 7) showing slower tumor progression in PTT-treated mice relative to untreated controls.

After completing the biodegradation, stability, and PTT characterization studies that demonstrated improved properties of the PBNPs at intratumoral pH, we conducted

studies evaluating the efficacy of PBNP-based PTT in treating aggressive tumors. For these studies, we utilized a syngeneic mouse Neuro2a model of neuroblastoma using Neuro2a cells, which have been previously demonstrated to exemplify an advanced or challenging tumor type. Specifically, 4-6-week old A/J mice were subcutaneously injected with 1 million luciferase-expressing bioluminescent Neuro2a cells in accordance with Children's National Health System's Institutional Animal Care and Use Committee (IACUC)-approved protocol. Tumor treatment was commenced when the animals reached a tumor size of at least 5 mm (~60 mm^3 volume) measured using both calipers and bioluminescence measurements. Due to the intrinsic variation in tumor engraftment, the mice were treated within a range of 3-5 days rather than on the same day. The tumor-bearing mice were either intratumorally injected with 50 μL of 1 mg/mL PBNPs and irradiated with an 808 nm laser (1.875 W/cm^2 for 10 minutes) or left untreated (**Fig. 4**). Tumor bioluminescence was measured every two days to assess the efficacy of the treatment or tumor progression (**Fig. 4A-B**). Mice in the PTT-treated group exhibited near complete tumor eradication immediately after treatment (minimal measured bioluminescence; **Fig. 4A**) compared with mice in the untreated, control group that exhibited consistent tumor progression and growth (increased in measured bioluminescence; **Fig. 4B**). Aggregate data from multiple tumor progression studies showed that when tumor-bearing mice where treated with PTT, their tumors were eradicated almost completely, and that the mice in this group had an average of 3 tumor-free days before they reappeared (**Fig. 4C**). Furthermore, although the tumors relapsed, the tumor progression was slower in these mice compared with mice in the untreated, control group, which exhibited a rapid increase in tumor volume. Our results indicate the

efficacy of PBNP-based PTT in effecting rapid tumor debulking, increasing the number of tumor-free days, and decreasing tumor growth rates in neuroblastoma tumor-bearing mice. Despite this, PBNP-based PTT therapy did not generate sustained tumor eradication, and the tumors eventually reappeared.

2.3.4 Effect of Prussian blue nanoparticle-based photothermal therapy on stimulating a T cell-mediated response.

The incomplete responses to PBNP-based PTT seen in neuroblastoma-bearing mice prompted us to investigate therapies that could be combined synergistically with PTT to confer long-term survival. Specifically, we sought therapies that exploited the immune system, as they offer the potential for improved treatment outcomes and conferring immunity against disease recurrence by harnessing molecular and cellular components of the complex immune system. Additional impetus for exploring immunotherapy in combination with PTT came by way of earlier reports demonstrating the immunostimulatory effects of nanoparticle-based PTT.[20, 31-32] We decided to pursue checkpoint blockade immunotherapy in particular for our combination with PBNP-based PTT given the growing body of evidence demonstrating its role in significantly improving survival in patients with advanced cancers in clinical trials.[69-73] We selected anti-CTLA-4 as it was the first FDA-approved checkpoint blockade immunotherapy (ipilimumab). Anti-CTLA-4 reverses T cell exhaustion, unleashing their potent antitumor effects. Therefore, we investigated the ability of PBNP-based PTT to stimulate a T cell-mediated response, as that would provide the rationale for exploring it in combination with anti-CTLA-4.

We conducted studies quantifying the relative proportions of tumor infiltrating lymphocytes after PTT. As described previously, neuroblastoma-tumor bearing mice were divided into two groups: PTT-treated and untreated controls. To measure the tumor expression levels of lymphocytes and specifically T cells after PTT, mice were sacrificed 24 h and 96 h post-treatment and their tumors (or residual tumors in case of tumor shrinkage) were isolated. Tumors were processed to obtain single cell suspensions and analyzed using flow cytometry for CD45 (lymphocyte) and CD3 (T cell) expression. After 24 h, there was no significant difference in lymphocyte and T cell populations in the treated versus untreated tumors (**Fig. S3**). However, 96 h post-treatment, the tumors in PTT-treated mice exhibited a significant increase in lymphocyte (i.e. average values of CD45+; 9.7% PTT-treated vs. 4.1% untreated; **Fig. 5A-C**) and T cell (i.e. average values of CD3+; 6.2% PTT-treated vs. 2.2% untreated; **Fig. 5D-F**) infiltration. These results suggest an increased recruitment of T cells to the tumor site after PTT given the appropriate time scale.

Next, we investigated whether PTT resulted in global activation of T cells, necessary for mounting a robust systemic antitumor immune response. For these studies, T cells were isolated from the spleens of PTT-treated and untreated mice (using mouse T cell-specific CD5 immunomagnetic beads) were co-cultured with tumor stimuli for evaluation of IFN γ production (a cytokine produced by activated T cells)[74-75] using an ELISpot assay (**Fig. 5G**). Although the mean IFN γ secretion levels from the isolated splenocytes following stimulation with control Neuro2a tumor cells were higher in the PTT-treated group compared to the untreated group, this was largely due to the fact that two out of the five mice in the group secreted significantly higher levels of IFN γ ; the other three mice

in this group secreted basal levels. By contrast, none of the mice in the untreated group secreted significantly elevated levels of IFN γ . Taken together, our results suggest that PTT alone can stimulate a T cell-mediated response, although these effects may not be strong enough to eradicate advanced cancers

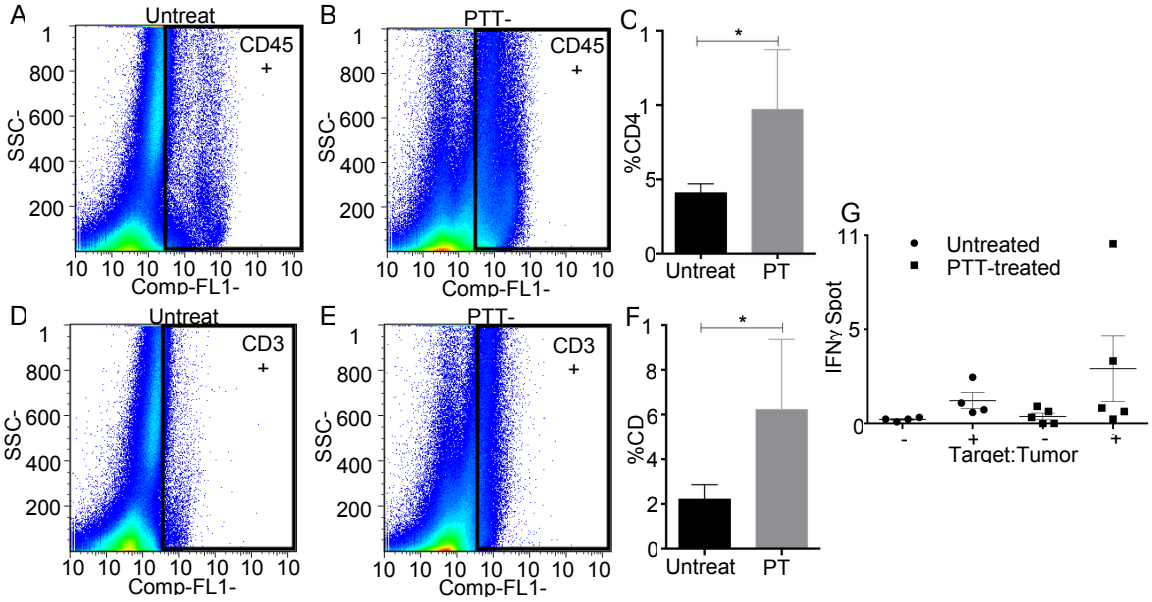

Figure 5. Effect of PBNP-based PTT on stimulating a T cell-mediated response. Representative scatter plots of CD45 positive tumor cells in A) Untreated and B) PTT-treated mice. C) Percentage of CD45+ cells in the tumors of untreated (n= 4) and PTT-treated (n=5) mice showing significantly higher percentage of CD45+ cells in tumors of PTT-treated relative to untreated mice (9.70% vs. 4.09%, p-value = 0.0294). Representative scatter plots of CD3 positive tumor cells in D) Untreated and E) PTT-treated mice. F) Percentage of CD3+ cells in the tumors of untreated (n= 4) and PTT-treated (n=5) mice showing significantly higher percentage of CD3+ cells in tumors of PTT-treated relative to untreated mice (6.22% vs. 2.21%, p-value = 0.0424). G) Interferon gamma (IFNγ) ELISpot using splenocytes from PTT-treated and untreated mice. PTT-treated mice splenocytes exhibited increased expression of IFNγ following re-exposure to Neuro2a cells in a subset of mice (2/5) compared to untreated mice, which showed no response (0/4)

2.3.5 Effect of the combination photothermal immunotherapy on tumor regression and long-term survival.

In order to increase the antitumor immune response for improved therapeutic outcomes in our mouse neuroblastoma model, we used anti-CTLA-4 immunotherapy in combination with PBNP-based PTT to decrease immunosuppression and unleash the killing potential of activated T cells. We conducted studies investigating the efficacy of this combination photothermal immunotherapy. Specifically, neuroblastoma tumor-bearing mice (~60 mm^3 tumor volumes) were divided into four groups (**Table 1**): 1) PTT + anti-CTLA-4 group (n=9): which received intratumoral PTT and i.p. anti-CTLA-4, 2) PTT group (n=6): which received intratumoral PTT, 3) anti-CTLA-4 group (n=8): which received i.p. anti-CTLA-4 , and 4) Untreated group (n=10): where the mice were not subject to any treatment. We monitored both the tumor progression through bioluminescent imaging, and the long-term survival of the mice.

Table 1. Groups and treatments used in the study.

Group (# mice)	Treatment
PTT*+anti-CLTA-4# (n=9)	PTT on Day 0; anti-CTLA-4 on Days 1, 4, 7
PTT* (n=6)	PTT on Day 0
anti-CTLA-4# (n=8)	anti-CTLA-4 on Days 0, 3, 6
Untreated (n=10)	No treatment
* PTT-treated groups receive 50 µL of 1 mg/mL PBNPs intratumorally, irradiated by an 808 nm laser at 1.875 W/cm^2 for 10 minutes	
# anti-CTLA-4-treated groups receive 150 µg of anti-CTLA-4 per dose by i.p. injection	

A representative temporal image measuring the tumor-specific bioluminescence indicated a gradual decrease in tumor size and subsequent elimination of the tumor in a mouse treated with our combination photothermal immunotherapy (**Fig. 6A**). Further, the tumor

progression was significantly slower in the combination PBNP-based PTT + anti-CTLA-4 group when compared with untreated controls (**Fig. 6B**). Most importantly, the combination therapy resulted in complete tumor regression and long-term survival in 55.5% of the treated mice (**Fig. 6C and S4**). The long-term, tumor-free survival was significantly higher (determined by a log-rank test) than that observed for mice treated with anti-CTLA-4 alone (12.5%), PTT (0%), or left untreated (0%). The results suggest that the PTT caused the initial reduction in tumor burden, which was complemented by the anti-CTLA-4 treatment which targeted and eliminated residual tumor cells, conferring long-term tumor-free survival in the combination therapy-treated mice. Our results also suggest the potential of our combination therapy to confer long-term survival in advanced cancers.

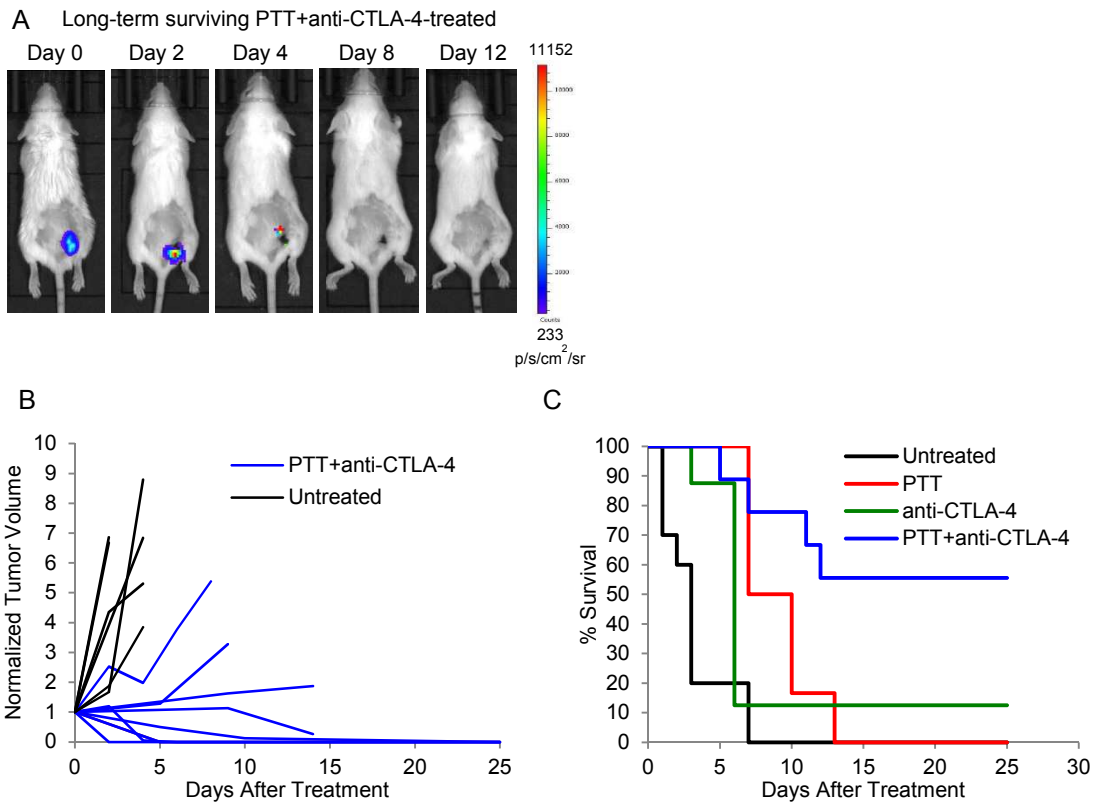

Figure 6. Effect of the combination therapy (combined PTT+anti-CTLA-4 therapy) on tumor regression and long-term survival in the neuroblastoma mouse model. A) Representative image of a long-term surviving mouse treated with PTT+anti-CTLA-4 showing tumor regression (decrease in bioluminescence, measured on the same scale for multiple days) and fading of the PTT-induced scar. Scale bar on the right represents the bioluminescence intensity measured in p/s/cm^2/sr. B) Normalized tumor growth curves for tumor-bearing mice treated with PTT+anti-CTLA-4 (blue) or left untreated (black). 55% of the mice treated with PTT+anti-CTLA-4 survived tumor-free. C) Kaplan-Meier survival plots of neuroblastoma mice that were treated with PTT+anti-CTLA-4 (n=9), anti-CLTA-4 alone (n=8), PTT alone (n=6), or untreated (n=10). Mice receiving the combination therapy showed significantly higher long-term survival (> 100 days, not plotted above so as to observe changes in survival within the other groups) compared with mice in the other groups (determined by a log-rank test; $p < 0.05$).

2.3.6 Effect of tumor rechallenge on long-term surviving mice that were previously treated with photothermal immunotherapy.

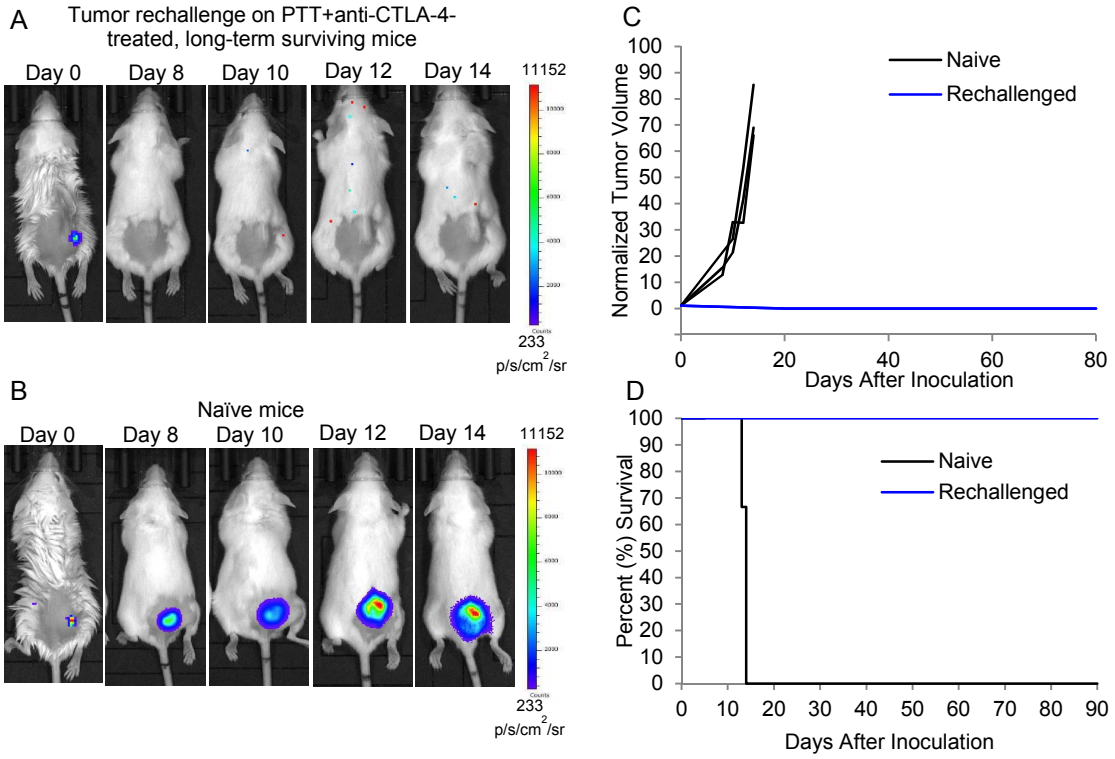

Figure 7. Effect of tumor rechallenge in combination photothermal immunotherapy-treated, long-term surviving mice. Representative images showing protection against tumor rechallenge in A) combination therapy treated mice (n=3) and B) progression of tumor in naïve, untreated mice (n=3). Scale bar represents the bioluminescence intensity measured in p/s/cm^2/sr. C) Tumor growth curves after challenge with 10^6 neuroblastoma cells in untreated mice (naïve, black; n=3) and long-term surviving combination therapy-treated mice (rechallenged, blue; n=3). When the mice were previously treated with the combination therapy (blue), they all survived tumor-free, compared to the controls (black), which rapidly grew tumors after challenge (inoculation). D) Kaplan-Meier survival plots of rechallenged and naïve mice. Mice in the rechallenged group showed significantly higher long-term survival compared to naïve mice (determined by a log-rank test, $p < 0.05$).

An ideal tumor therapy would be one that not only effectively eradicates tumors but prevents recurrence after their successful elimination from the body. We conducted studies to investigate whether our combination therapy conferred protection in long-term surviving mice that are rechallenged with the original tumor cells (Neuro2a). Our studies consisted of two groups: 1) naïve group (n=3): where mice were challenged with 10^6 Neuro2a cells and 2) rechallenged group (n=3): where long-term surviving mice

previously treated with the combination therapy were rechallenged with 10^6 Neuro2a cells after at least 90 days of tumor-free survival. Remarkably, all of the long-term surviving mice exhibited protection against tumor rechallenge; the mice rapidly eliminated the rechallenged tumors (**Fig. 7A and S5**), compared with consistent tumor progression post-challenge in the naïve mice (**Fig. 7B and S5**).

Tumor volumes in the rechallenged mice rapidly disappeared in contrast with the tumor progression observed in the naïve mice (**Fig. 7C**). The rechallenged mice went on to survive for more than 90 days post tumor rechallenge compared with naïve mice that had to be sacrificed due to high tumor burden 12-14 days post-challenge (**Fig. 7D**). These data suggest the potential of the combination therapy in conferring tumor immunity and protection in long-term surviving mice against tumor rechallenge/recurrence.

2.4 Discussion

We have described a novel combination therapy termed photothermal immunotherapy that combines PBNP-based PTT with anti-CTLA-4 checkpoint blockade immunotherapy (**Fig. 1**) for treating advanced tumors. As synthesized by us, PBNPs exhibited an inherent pH-dependent degradation (**Fig. 2A-C**) and stability (**Fig. 2D**) where they were stable at acidic pH mimicking conditions observed in the interstitia of tumors, and exhibited incipient degradation and instability at higher pH mimicking blood/lymph. Importantly, the degradation products were not observed to exhibit cytotoxicity (**Fig. 2E**) under the conditions tested. Harnessing the pH gradient of tumor interstitia relative to surrounding tissue is an intriguing strategy to selectively trigger and/or control tumor treatment.[76-77] Tumor interstitia are typically acidic, due to the hypoxia and lactic acid accumulation that rapidly occurs in a growing tumor.[78] Our *in vitro* data demonstrating that PBNPs exhibit

properties strongly dependent on the pH of the environment suggest their potential for use in delivering tumor-specific therapies, where the PBNPs remain intact and stable intratumorally, while rapidly and safely degrading when they enter the bloodstream or lymphatic system, thereby minimizing potential toxicities to normal cells – an important consideration in the field of nanomedicine for eventual clinical translation. The pH-dependent properties of PBNPs had a significant effect on their PTT capabilities; PTT capabilities were decreased at blood/lymph pHs relative to intratumoral pHs (**Fig. 3A**). This led us to establish the concentrations of PBNPs intratumorally administered to ensure that there were sufficient nanoparticles intratumorally to effect tumor ablation (**Fig. 3B**). It is likely that similar optimization studies will have to be carried out should the conditions under which PTT is administered is changed, e.g. superficial versus deeper tumors may require different nanoparticle doses, laser power densities, and/or duration of irradiation. It is important to state here that should the need arise for PBNPs to exhibit longer temporal stability and significantly slower degradation kinetics than that observed (especially in applications that require intravenous administration), the PBNPs can be appropriately surface-coated with biocompatible polymers such as polyethylene glycol, as previously described.[79]

PBNP-based PTT in our mouse model for an antigenic but aggressive cancer (the syngeneic Neuro2a model of neuroblastoma) demonstrated an incomplete response in tumor-bearing mice relative to untreated mice (**Fig. 4**), although it significantly decreased tumor burden immediately after PTT, and decreased tumor growth rates (**Fig. 4**). As described previously, PTT confers long-term, tumor-free survival in multiple animal models of cancer premised on the observation that cancer cells are more susceptible to

heat than normal tissue because of their elevated metabolic rates.[80-81] However, in the case of aggressive cancers, such as our neuroblastoma model, we suspect that PTT does not eliminate all cancer cells even when they are undetectable by bioluminescence or caliper measurements. The nascent cancer cells likely grow into new tumors, similar to clinical observations in neuroblastoma.[82] It is possible that residual cancer cells remain even in other tumor models that show complete remission. We speculate that in those cases, the residual tumor cells may be cleared by a robust immune response.

PBNP-based PTT resulted in increased T cell infiltration into the tumor regions (**Fig. 5**). Lymphocytes found in tumors have been shown to be effective at delaying tumor progression, suggesting their potential influence on improved patient prognosis.[83-86] Therefore, the increased population of CD45+ cells (**Fig. 5A-C**) in the residual tumors of PTT-treated mice presents an opportunity to recruit these cells for tumor eradication.[87] Within this subset of lymphocytes, T cells are also present in increased numbers (CD3+ cells; **Fig. 5D-F**) and similarly present an opportunity to recruit this subset of immune effector cells to generate a T cell mediated antitumor response.[88] Furthermore, results from our IFN γ ELISpot indicate that a subset of PTT-treated mice (40%) exhibited increased systemic T cell function as compared to untreated mice. IFNγ is produced by a wide variety of immune cells including T lymphocytes once immune activation and antigen specific immunity is initiated.[74] Therefore, its upregulation in a subset of mice indirectly reflects the role of PTT in generating tumor antigens or providing an *in situ* vaccination effect, important for generating a robust antitumor immune response. Our studies thus demonstrate that PTT not only ablates the tumors, but elicits a T cell-mediated immune response, which alone cannot prevent tumor relapse or recurrence

likely due to the immunosuppressive mechanisms[89-90] exerted by tumor cells to evade T cell-mediated responses.

PTT in combination with anti-CTLA-4 immunotherapy resulted in complete tumor regression and long-term survival in 55.5% of the tumor-bearing mice compared to only 12.5% survival observed in mice treated with anti-CTLA-4 alone and 0% survival observed in both mice treated with PTT alone or left untreated (**Fig. 6**). We attribute this significantly higher long-term survival benefit in the combination therapy-treated mice to the reversal of T cell exhaustion and immunosuppression by anti-CTLA-4, which is complemented by the debulking and priming of a T cell-mediated response by PTT. Previous studies using the Neuro2a mouse model have demonstrated higher long-term survival using anti-CTLA-4 alone than observed in this study (~40-50% vs. 12.5% in our study).[30, 52] The difference between these observations can potentially be attributed to the fact that the earlier studies commenced the anti-CTLA-4 immunotherapy when their mice reached tumor sizes of ~1 mm or after a fixed number of days (typically 5-6 days) after tumor inoculation, while we commenced the therapy only after tumors reached ~5 mm, thus potentially reflecting a significantly higher tumor burden and disease progression in our studies. Finally, long-term surviving mice treated with the combination therapy exhibited protection against tumor rechallenge indicating the development of immunity against these tumors in the combination therapy-treated mice (**Fig. 7**). However, further studies are necessary to elucidate the underlying immunological mechanisms that elicit these protective responses.

In summary, this body of work represents one of the first studies that exploit multifunctional nanoparticles in combination with immunotherapy in the field of cancer

therapy. Our work points to the important role that PBNPs (and other nanoparticle platforms) may play in the upcoming years in immunoengineering,[91] where nanoparticles are used to engineer a suitable immune response to treat advanced cancers.

Chapter 3: Conclusions

3.1 Summary

We have described biodegradable PBNPs that were used in combination with anti-CTLA-4 immunotherapy for treating mice in an aggressive model of neuroblastoma. Our PBNPs exhibit pH-dependent degradation and stability, where they are stable at lower pH mimicking the intratumoral milieu and degrade at mildly alkaline pH mimicking blood/lymph. PTT by itself was observed to confer only a marginal survival benefit in mice with neuroblastoma, but resulted in a robust infiltration of lymphocytes and activation of systemic (splenic) T cells against tumor cells. Finally, mice treated with combination PTT and checkpoint inhibition exhibited significantly tumor regression and long-term tumor immunity. Our results showcase the potential for the use of PBNP-based PTT in combination with checkpoint blockade immunotherapy in treating advanced cancers, and these proof-of-concept studies should serve as an important prelude to further clinical translation.

3.2 Contributions to the field

This project utilizes Prussian blue nanoparticles for photothermal therapy (PTT) in combination with anti-CTLA-4 checkpoint blockade immunotherapy to treat neuroblastoma in a mouse model. The innovative aspects of our approach and contributions to the field include:

3.2.1 Use of biodegradable Prussian blue nanoparticles for photothermal therapy of neuroblastoma. Prussian blue nanoparticle-based photothermal therapy is a minimally invasive, *in situ* method for destroying cancer cells and reducing tumor burden. As compared to other nanoparticles that have been used for PTT, we have the ability to

synthesize Prussian blue nanoparticles that are stable in tumor environments, and safely biodegrade in physiological media (from hours to weeks), thus mitigating concerns associated with the long-term fate and toxicity of these nanoparticles within the body. Further, Prussian blue nanoparticles can be easily synthesized in a scalable manner with a single-step at low costs, and is already FDA approved for human oral use.

When compared to the current state of the art in hyperthermia and thermal ablation methods, Prussian blue nanoparticle-based PTT offers enormous flexibility. Our Prussian blue nanoparticles can be easily modified for multiple functions such as biofunctionalization for immunomodulatory or therapeutic molecules; an advantage not offered by alternative hyperthermia or thermal ablation methods.

3.2.2 Prussian blue nanoparticle-based photothermal therapy offers a vaccination effect that elicits a T-cell based response. The release of key tumor antigens and "danger signals" that fight against the tumor are a result of PTT-based destruction of neuroblastoma cells. This release provides an immunostimulatory, multi-antigen vaccination effect without the need for knowledge on specific tumor antigen targets, as required for standard vaccines. As compared with other nanoparticles in the field such as carbon nanotubes, and gold nanoparticles, the immune response elicited by Prussian blue nanoparticles is solely based on PTT, and not on a side effect from the toxicity of these nanoparticles, making it ideal for combining it with an immunotherapy such as checkpoint blockade, due to the increased infiltration of T-cells that will aid in starting a robust anti-tumor immune response.

3.2.3 Use of anti-CTLA-4 for checkpoint blockade immunotherapy in conjunction with Prussian blue nanoparticle-based photothermal therapy. We are one of the first groups to

demonstrate the use of a checkpoint inhibitor with photothermal therapy for the treatment of advanced cancers. Our novel photothermal immunotherpy expands the field of cancer therapies because as demonstrated by our results, photothermal immunotherapy is more effective than either immunotherapy or photothermal therapy alone against primary treated tumor in a mouse model of neuroblastoma. It has been shown that photothermal ablation of cancer cells alone is not enough to provide the patient protection against metastatic or distal tumors. Additionally, clinical reports on the use of ipilimumab showed that patients responsed poorly to this treatment alone. This is because some tumors are poorly immunogenic and hardly eny endogenouse tumor-specific T cells are stimulated before intervention. By combinting photothermal heating with checkpoint-blockade immunotherapy, it elicits stronger immune responses against the tumor, increasing the response rate in patients. Although the mechanistic details remain to be investigated, the therapeutic effects shown by PTT and anti-CTLA-4 are very encouraging. Further efforts should now be focused on enhancing treatment protocols for clinical trials to improve efficacy.

3.3 Future directions

The findings here suggest that photothermal immunotherapy results in complete tumor regression and long-term survival in a significantly higher proportion of mice (56%) in the standard Neuro2a model of neuroblastoma. The next projects will evaluate the combination therapy in aggressive (AgN2a, an aggressive subclone of Neuro2a) model of cancer, where the therapeutic outcomes will be compared to standards of care for neuroblastoma: surgery, chemotherapy, and anti-GD2 immunotherapy.

Efficacy studies in an aggressive model of neuroblastoma will be conducted in the future since it poses critical hurdles for treatment: it is less immunogenic,[52] can adapt to its environment[92] and it is capable of subverting the immune response, making it harder to treat. These criteria are all met by the AgN2a mouse model, which should ensure a more objective evaluation of the therapeutic potential of our photothermal immunotherapy strategy.

Additionally, we will study the effects of PTT itself on the antitumor immune response by developing a "PTT vaccine" comprised of injected PTT-treated AgN2a cells, alone and in combination with anti-CTLA-4. This will answer our question of whether or not PTT serves the dual purpose of rapidly reducing tumor burden and generating a multi-antigen vaccination effect.

The mechanisms of prolonged immune protection will be further studied in the aggressive model of neuroblastoma by studying the immunological memory against the target cells, and performing immune cell depletion studies where a single type of immune cell (NK, CD4, CD8) is depleted using intraperitoneally administered antibodies against the specific cell type. These studies may help elucidate the role of the various cell types in conferring prolonged immunity.

Lastly, we will biofunctionalize the Prussian blue nanoparticles with antibodies for targeting or with immunomodulatory or therapeutic molecules for further therapeutic functions. The modification of these nanoparticles will further help making them translatable into the clinic, by offering characteristics that will help make them better at targeting and treating cancers.

Supporting Information

Vis-NIR spectroscopy of the PBNPs; DLS of the PBNPs as a function of pH and time (day); Flow cytometry analysis of tumor infiltration 24 h after PTT; ELISpot analysis of splenic T-cell activation; Bioluminescent monitoring of tumor progression in PTT + anti-CTLA-4, anti-CTLA-4, PTT, and untreated mice; Bioluminescent monitoring of tumor progression in rechallenged and naïve mice.

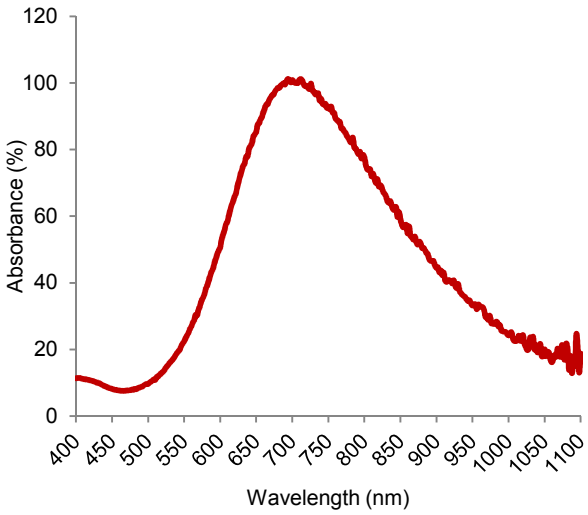

Figure S1. Vis-NIR spectrum of PBNPs. PBNPs were analyzed using the VISIONlite software on the Genesys 10S spectrophotometer (Thermo Scientific, Waltham, MA).

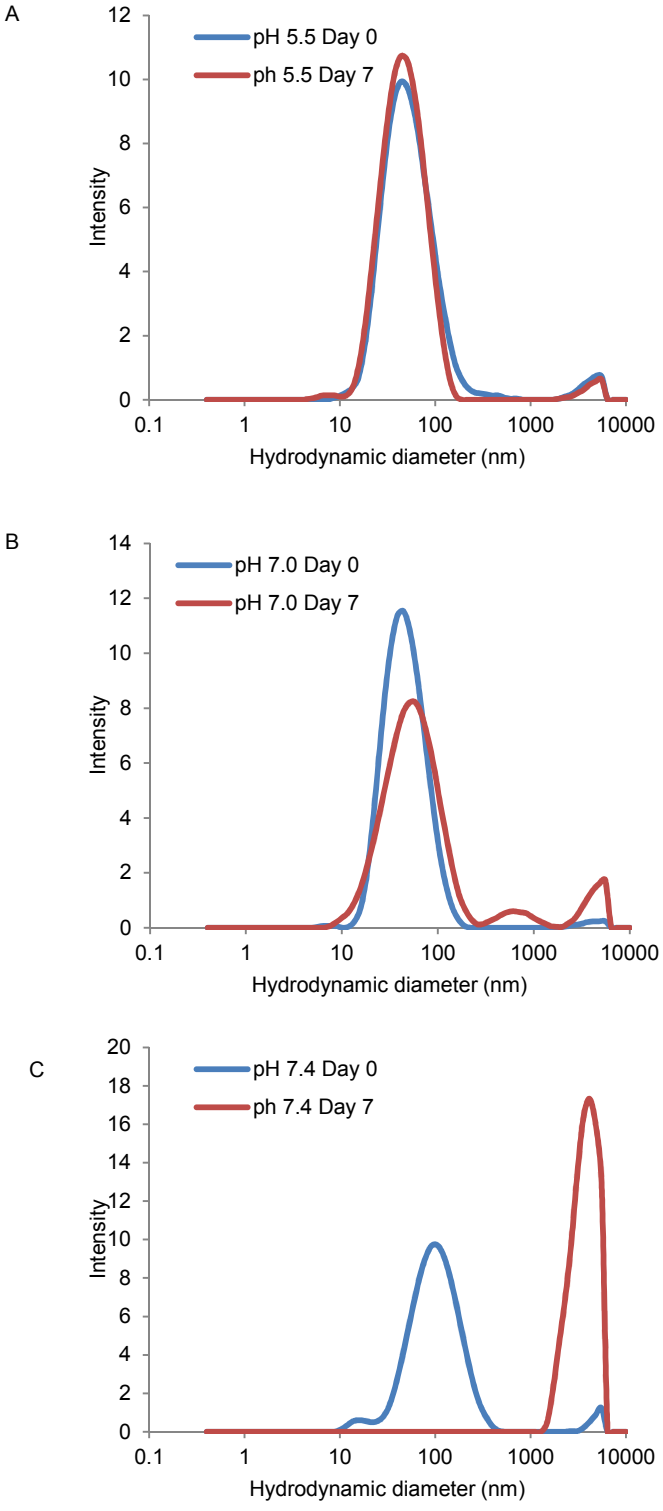

Figure S2. Hydrodynamic diameter intensity distributions of PBNPs in varied pH. PBNP sizes were quantified by dynamic light scattering (DLS) over 7 days (Day 0: blue, Day 7: red) at pH A) 5.5, B) 7.0, and C) 7.4, illustrating stability at mildly acidic/neutral pHs that mimic tumor interstitia and instability at mildly alkaline pHs (7.4) mimicking the lymph and blood.

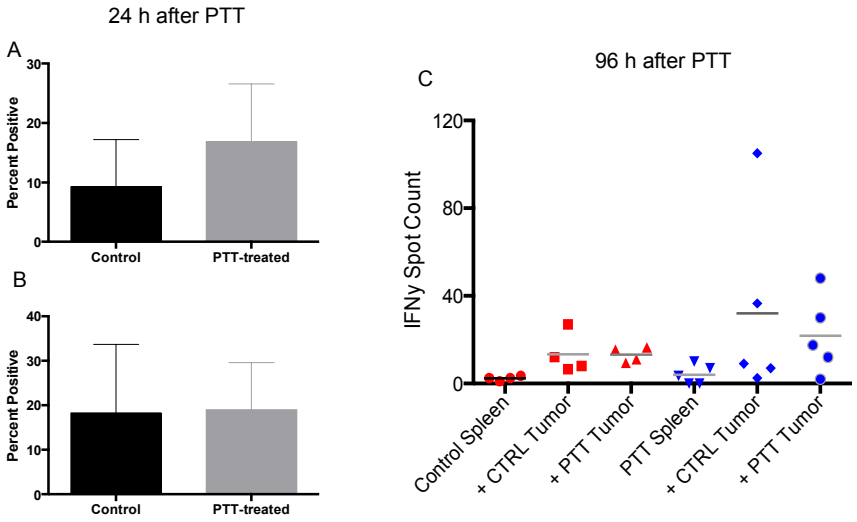

Figure S3. Effect of PBNP-based PTT on stimulating a T cell-mediated response. A) Percentage of CD3+ cells in the tumors of untreated (n= 4) and PTT-treated (n=5) mice statistically insignificant differences between the two groups. B) Percentage of CD45+ cells in the tumors of untreated (n= 4) and PTT-treated (n=5) mice also showing statistically insignificant differences between the two groups. C) Interferon gamma (IFN□) ELISpot using splenocytes from PTT-treated and untreated mice re-exposed to Neuro2a tumors cells (+CTRL tumor) or pooled PTT tumor cells (+ PTT tumor).

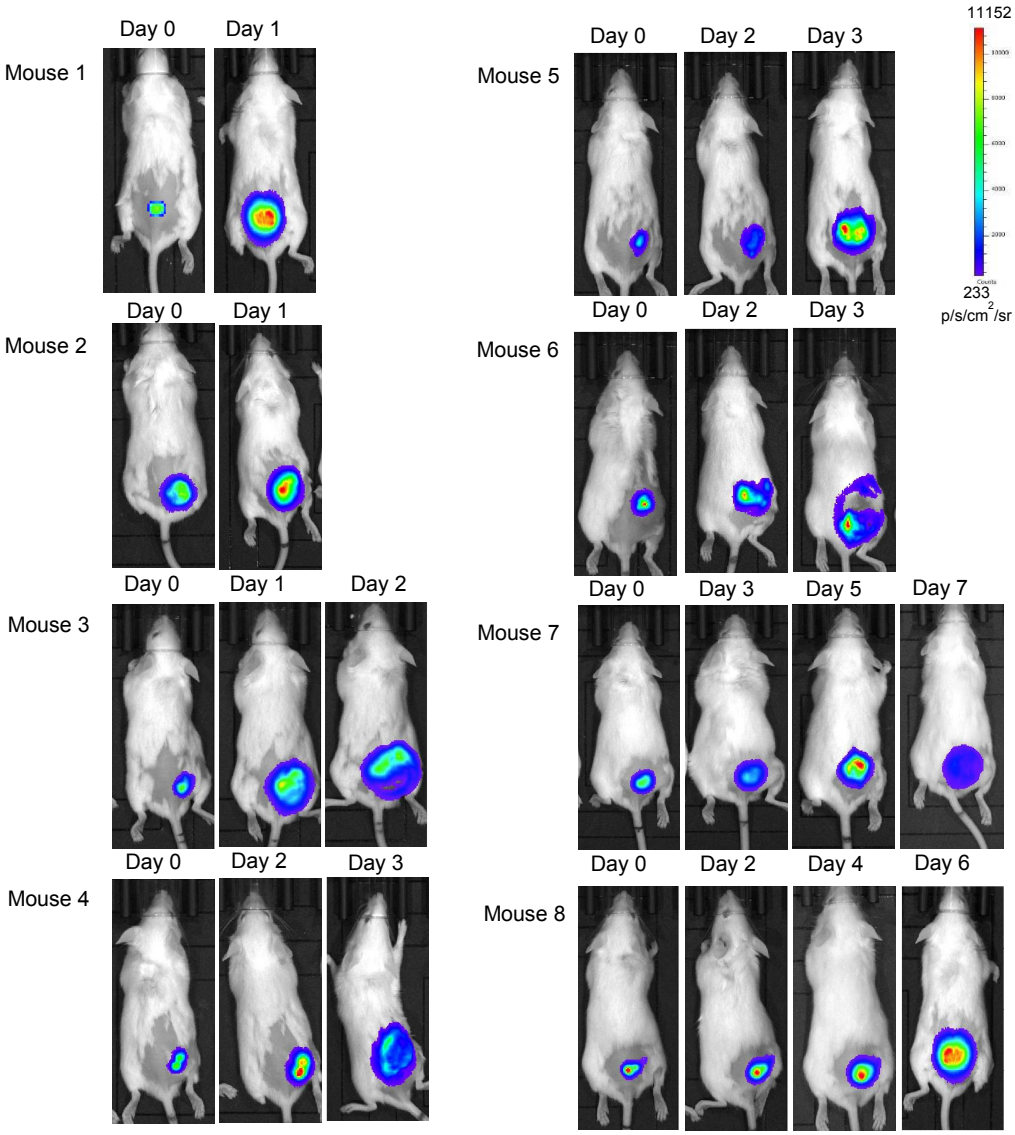

Figure S4A. Representative images of untreated tumor-bearing mice. Scale bars on the panel represent the bioluminescent intensity in p/s/cm^2/sr.

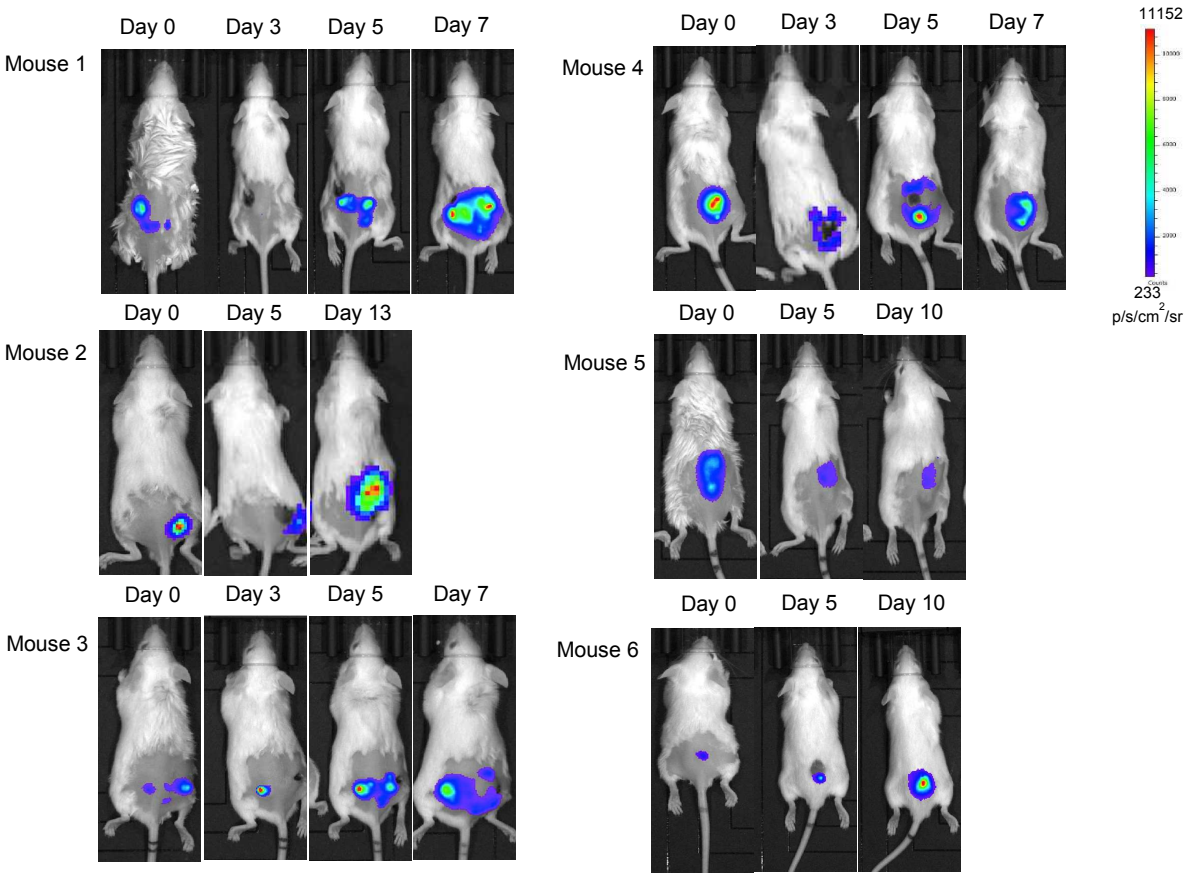

Figure S4B. Representative images of tumor-bearing mice that were treated with photothermal therapy (PTT). Scale bars on the panel represent the bioluminescent intensity in p/s/cm^2/sr.

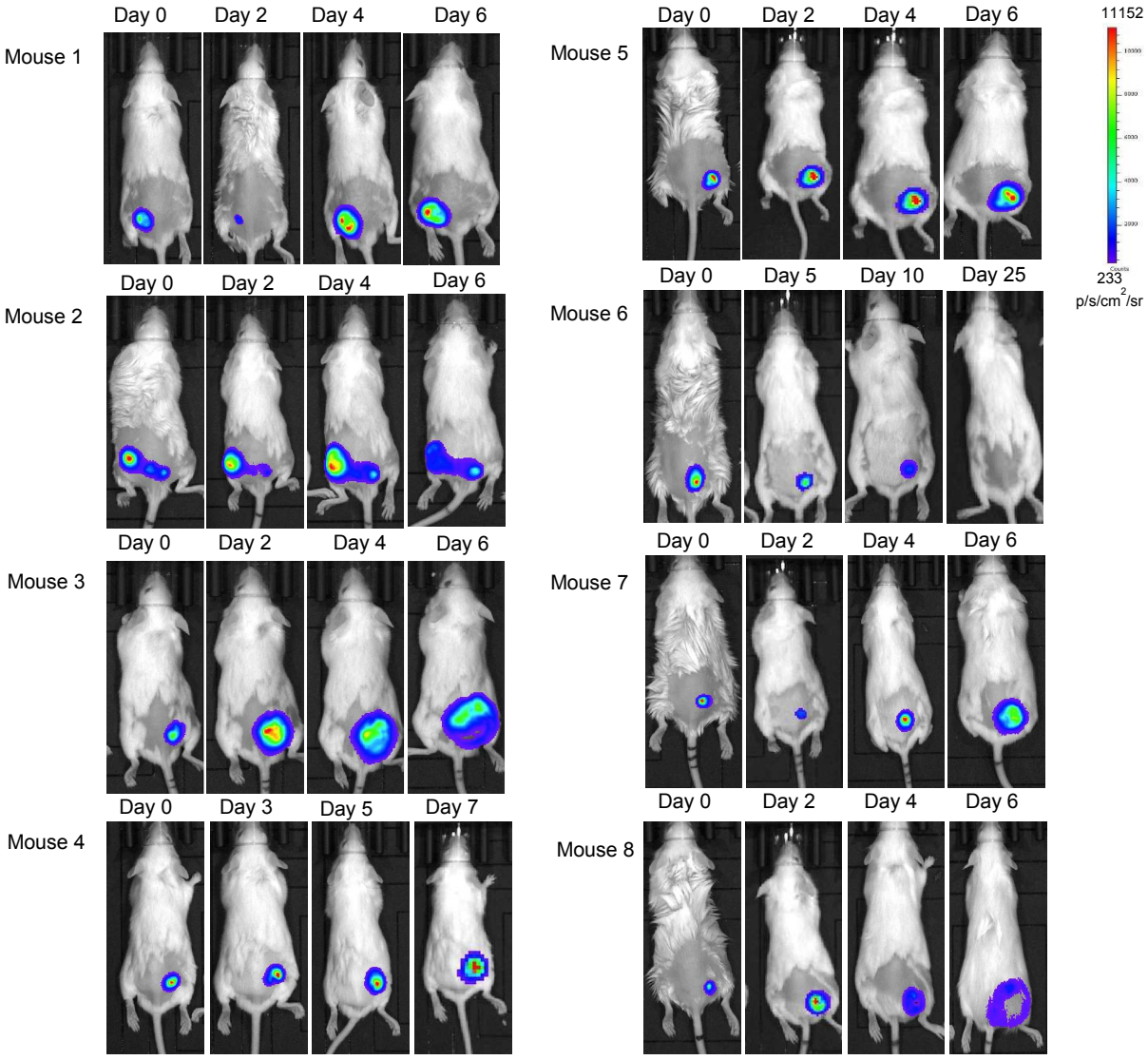

Figure S4C. Representative images of tumor-bearing mice that were treated with anti-CTLA-4 therapy. Scale bars on the panel represent the bioluminescent intensity in p/s/cm^2/sr.

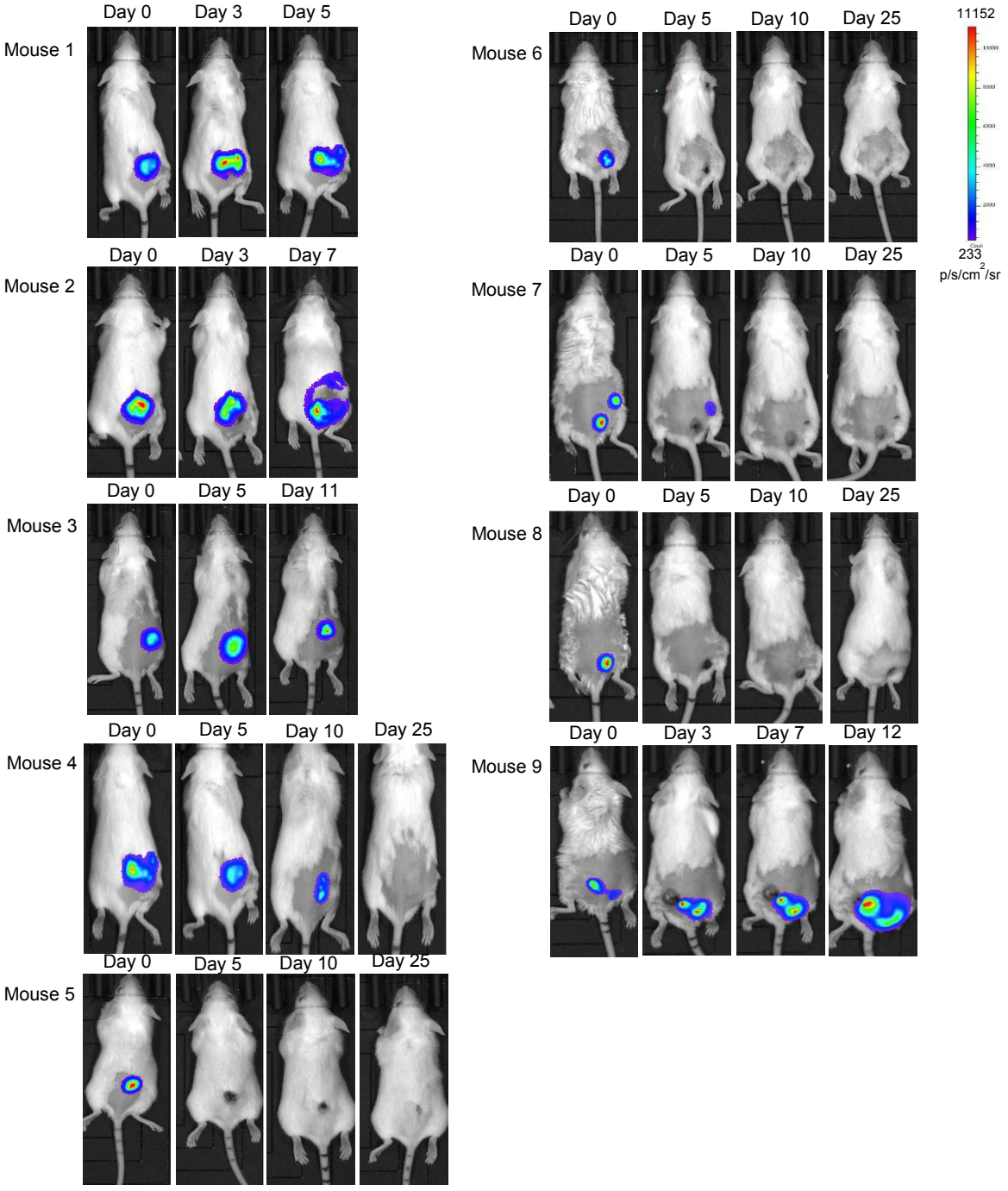

Figure S4D. Representative images of tumor-bearing mice that were treated with the combination photothermal immunotherapy. Scale bars on the panel represent the bioluminescent intensity in p/s/cm^2/sr.

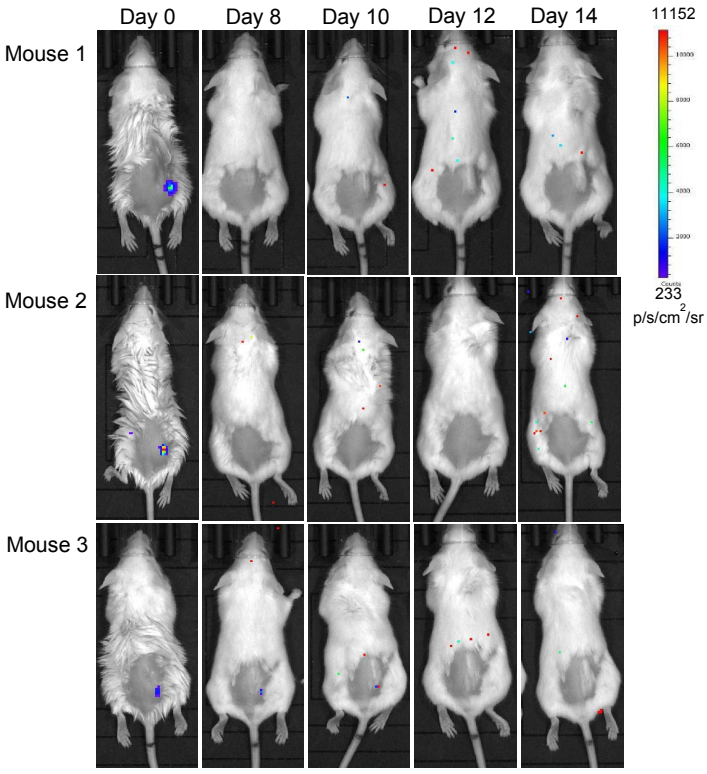

Figure S5. Representative images showing protection against tumor rechallenge in combination therapy treated mice (n=3). Scale bar represents the bioluminescence intensity measured in p/s/cm^2/sr.

Bibliography

1. Siegel, R. L.; Miller, K. D.; Jemal, A., Cancer statistics, 2015. *CA Cancer J Clin* **2015,** *65* (1), 5-29.
2. Ward, E.; Desantis, C.; Robbins, A.; Kohler, B.; Jemal, A., Childhood and adolescent cancer statistics, 2014. *CA Cancer J Clin* **2014,** *64* (2), 83-103.
3. Brodeur, G. M.; Hogarty, M. D.; Mosse, Y. P.; Maris, J. M., Neuroblastoma. In *Principles and Practice of Pediatric Oncology*, 6th ed.; Pizzo, P. A.; Poplack, D. G., Eds. Wolters Kluwer Health/Lippincott Williams & Wilkins: Philadelphia, PA, 2010; pp 886-922.
4. Bellanti, F.; Kågedal, B.; Della Pasqua, O., Do pharmacokinetic polymorphisms explain treatment failure in high-risk patients with neuroblastoma? *Eur J Clin Pharmacol* **2011,** *67 Suppl 1*, 87-107.
5. Maeda, H.; Wu, J.; Sawa, T.; Matsumura, Y.; Hori, K., Tumor vascular permeability and the EPR effect in macromolecular therapeutics: a review. *J Control Release* **2000,** *65* (1-2), 271-84.
6. Matsumura, Y.; Maeda, H., A new concept for macromolecular therapeutics in cancer chemotherapy: mechanism of tumoritropic accumulation of proteins and the antitumor agent smancs. *Cancer Res* **1986,** *46* (12 Pt 1), 6387-92.
7. Lammers, T.; Kiessling, F.; Hennink, W. E.; Storm, G., Drug targeting to tumors: principles, pitfalls and (pre-) clinical progress. *J Control Release* **2012,** *161* (2), 175-87.
8. Pirollo, K. F.; Chang, E. H., Does a targeting ligand influence nanoparticle tumor localization or uptake? *Trends Biotechnol* **2008,** *26* (10), 552-8.
9. Xie, J.; Lee, S.; Chen, X., Nanoparticle-based theranostic agents. *Adv Drug Deliv Rev* **2010,** *62* (11), 1064-79.
10. Hoffman, H. A.; Chakarbarti, L.; Dumont, M. F.; Sandler, A. D.; Fernandes, R., Prussian blue nanoparticles for laser-induced photothermal therapy of tumors. *RSC Advances* **2014,** *4* (56), 29729-29734.
11. Dumont, M. F.; Hoffman, H. A.; Yoon, P. R.; Conklin, L. S.; Saha, S. R.; Paglione, J.; Sze, R. W.; Fernandes, R., Biofunctionalized Gadolinium-Containing Prussian Blue Nanoparticles as Multimodal Molecular Imaging Agents. *Bioconjug Chem* **2014,** *25* (1), 129-137.
12. Dumont, M. F.; Yadavilli, S.; Sze, R. W.; Nazarian, J.; Fernandes, R., Manganese-containing Prussian blue nanoparticles for imaging of pediatric brain tumors. *Int J Nanomedicine* **2014,** *9*, 2581-95.
13. Vojtech, J. M.; Cano-Mejia, J.; Dumont, M. F.; Sze, R. W.; Fernandes, R., Biofunctionalized prussian blue nanoparticles for multimodal molecular imaging applications. *J Vis Exp* **2015,** (98), e52621.
14. Faustino, P. J.; Yang, Y.; Progar, J. J.; Brownell, C. R.; Sadrieh, N., et al., Quantitative determination of cesium binding to ferric hexacyanoferrate: Prussian blue. *J Pharm Biomed Anal* **2008,** *47* (1), 114-25.
15. Verzijl, J. M.; Joore, H. C.; van Dijk, A.; Wierckx, F. C.; Savelkoul, T. J.; Glerum, J. H., In vitro cyanide release of four prussian blue salts used for the treatment of cesium contaminated persons. *J Toxicol Clin Toxicol* **1993,** *31* (4), 553-62.

16. Yang, Y.; Faustino, P. J.; Progar, J. J.; Brownell, C. R.; Sadrieh, N., et al., Quantitative determination of thallium binding to ferric hexacyanoferrate: Prussian blue. *Int J Pharm* **2008,** *353* (1-2), 187-94.
17. den Brok, M. H.; Sutmuller, R. P.; van der Voort, R.; Bennink, E. J.; Figdor, C. G.; Ruers, T. J.; Adema, G. J., In situ tumor ablation creates an antigen source for the generation of antitumor immunity. *Cancer Res* **2004,** *64* (11), 4024-9.
18. Sabel, M. S.; Nehs, M. A.; Su, G.; Lowler, K. P.; Ferrara, J. L.; Chang, A. E., Immunologic response to cryoablation of breast cancer. *Breast Cancer Res Treat* **2005,** *90* (1), 97-104.
19. Wu, F.; Zhou, L.; Chen, W. R., Host antitumour immune responses to HIFU ablation. *Int J Hyperthermia* **2007,** *23* (2), 165-71.
20. Guo, L.; Yan, D. D.; Yang, D.; Li, Y.; Wang, X.; Zalewski, O.; Yan, B.; Lu, W., Combinatorial photothermal and immuno cancer therapy using chitosan-coated hollow copper sulfide nanoparticles. *ACS Nano* **2014,** *8* (6), 5670-81.
21. Tao, Y.; Ju, E.; Liu, Z.; Dong, K.; Ren, J.; Qu, X., Engineered, self-assembled near-infrared photothermal agents for combined tumor immunotherapy and chemo-photothermal therapy. *Biomaterials* **2014,** *35* (24), 6646-56.
22. Tao, Y.; Ju, E.; Ren, J.; Qu, X., Immunostimulatory oligonucleotides-loaded cationic graphene oxide with photothermally enhanced immunogenicity for photothermal/immune cancer therapy. *Biomaterials* **2014,** *35* (37), 9963-71.
23. Wu, M.; Wang, Q.; Liu, X.; Liu, J., Highly efficient loading of doxorubicin in Prussian Blue nanocages for combined photothermal/chemotherapy against hepatocellular carcinoma. *RSC Advances* **2015,** *5*, 30970-30980.
24. Xue, P.; Cheong, K. K.; Wu, Y.; Kang, Y., An in-vitro study of enzyme-responsive Prussian blue nanoparticles for combined tumor chemotherapy and photothermal therapy. *Colloids Surf B Biointerfaces* **2015,** *125*, 277-83.
25. Wolchok, J. D.; Kluger, H.; Callahan, M. K.; Postow, M. A.; Rizvi, N. A., et al., Nivolumab plus ipilimumab in advanced melanoma. *N Engl J Med* **2013,** *369* (2), 122-33.
26. Hodi, F. S.; O'Day, S. J.; McDermott, D. F.; Weber, R. W.; Sosman, J. A., et al., Improved survival with ipilimumab in patients with metastatic melanoma. *N Engl J Med* **2010,** *363* (8), 711-23.
27. Wolchok, J. D.; Chan, T. A., Cancer: Antitumour immunity gets a boost. *Nature* **2014,** *515* (7528), 496-8.
28. Schumacher, T. N.; Schreiber, R. D., Neoantigens in cancer immunotherapy. *Science* **2015,** *348* (6230), 69-74.
29. Carpentier, A. F.; Chen, L.; Maltonti, F.; Delattre, J. Y., Oligodeoxynucleotides containing CpG motifs can induce rejection of a neuroblastoma in mice. *Cancer Res* **1999,** *59* (21), 5429-32.
30. Williams, E. L.; Dunn, S. N.; James, S.; Johnson, P. W.; Cragg, M. S.; Glennie, M. J.; Gray, J. C., Immunomodulatory monoclonal antibodies combined with peptide vaccination provide potent immunotherapy in an aggressive murine neuroblastoma model. *Clin Cancer Res* **2013,** *19* (13), 3545-55.
31. Bear, A. S.; Kennedy, L. C.; Young, J. K.; Perna, S. K.; Mattos Almeida, J. P.; Lin, A. Y.; Eckels, P. C.; Drezek, R. A.; Foster, A. E., Elimination of metastatic

melanoma using gold nanoshell-enabled photothermal therapy and adoptive T cell transfer. *PLoS One* **2013,** *8* (7), e69073.
32. Wang, C.; Xu, L.; Liang, C.; Xiang, J.; Peng, R.; Liu, Z., Immunological responses triggered by photothermal therapy with carbon nanotubes in combination with anti-CTLA-4 therapy to inhibit cancer metastasis. *Adv Mater* **2014,** *26* (48), 8154-62.
33. Schutz, C. A.; Juillerat-Jeanneret, L.; Mueller, H.; Lynch, I.; Riediker, M., Therapeutic nanoparticles in clinics and under clinical evaluation. *Nanomedicine (Lond)* **2013,** *8* (3), 449-67.
34. Rink, J. S.; Plebanek, M. P.; Tripathy, S.; Thaxton, C. S., Update on current and potential nanoparticle cancer therapies. *Current opinion in oncology* **2013,** *25* (6), 646-51.
35. Results, S. E. a. E., SEER Stat Fact Sheets: Melanoma of the Skin. 2015.
36. Huang, X.; Jain, P. K.; El-Sayed, I. H.; El-Sayed, M. A., Plasmonic photothermal therapy (PPTT) using gold nanoparticles. *Lasers Med Sci* **2008,** *23* (3), 217-28.
37. Loo, C.; Lowery, A.; Halas, N.; West, J.; Drezek, R., Immunotargeted nanoshells for integrated cancer imaging and therapy. *Nano Lett* **2005,** *5* (4), 709-11.
38. Frangioni, J. V., In vivo near-infrared fluorescence imaging. *Curr Opin Chem Biol* **2003,** *7* (5), 626-34.
39. Weissleder, R., A clearer vision for in vivo imaging. *Nat Biotechnol* **2001,** *19* (4), 316-7.
40. Hirsch, L. R.; Stafford, R. J.; Bankson, J. A.; Sershen, S. R.; Rivera, B.; Price, R. E.; Hazle, J. D.; Halas, N. J.; West, J. L., Nanoshell-mediated near-infrared thermal therapy of tumors under magnetic resonance guidance. *Proc Natl Acad Sci U S A* **2003,** *100* (23), 13549-54.
41. Lal, S.; Clare, S. E.; Halas, N. J., Nanoshell-enabled photothermal cancer therapy: impending clinical impact. *Acc Chem Res* **2008,** *41* (12), 1842-51.
42. Dickerson, E. B.; Dreaden, E. C.; Huang, X.; El-Sayed, I. H.; Chu, H.; Pushpanketh, S.; McDonald, J. F.; El-Sayed, M. A., Gold nanorod assisted near-infrared plasmonic photothermal therapy (PPTT) of squamous cell carcinoma in mice. *Cancer Lett* **2008,** *269* (1), 57-66.
43. Au, L.; Zheng, D.; Zhou, F.; Li, Z. Y.; Li, X.; Xia, Y., A quantitative study on the photothermal effect of immuno gold nanocages targeted to breast cancer cells. *ACS Nano* **2008,** *2* (8), 1645-52.
44. Cobley, C. M.; Au, L.; Chen, J.; Xia, Y., Targeting gold nanocages to cancer cells for photothermal destruction and drug delivery. *Expert Opin Drug Deliv* **2010,** *7* (5), 577-87.
45. Kam, N. W.; O'Connell, M.; Wisdom, J. A.; Dai, H., Carbon nanotubes as multifunctional biological transporters and near-infrared agents for selective cancer cell destruction. *Proceedings of the National Academy of Sciences of the United States of America* **2005,** *102* (33), 11600-5.
46. Yu, J. G.; Jiao, F. P.; Chen, X. Q.; Jiang, X. Y.; Peng, Z. G.; Zeng, D. M.; Huang, D. S., Irradiation-mediated carbon nanotubes' use in cancer therapy. *J Cancer Res Ther* **2012,** *8* (3), 348-54.
47. Burke, A. R.; Singh, R. N.; Carroll, D. L.; Wood, J. C.; D'Agostino, R. B., Jr.; Ajayan, P. M.; Torti, F. M.; Torti, S. V., The resistance of breast cancer stem cells to

conventional hyperthermia and their sensitivity to nanoparticle-mediated photothermal therapy. *Biomaterials* **2012,** *33* (10), 2961-70.
48. Huang, N.; Wang, H.; Zhao, J.; Lui, H.; Korbelik, M.; Zeng, H., Single-wall carbon nanotubes assisted photothermal cancer therapy: animal study with a murine model of squamous cell carcinoma. *Lasers in surgery and medicine* **2010,** *42* (9), 638-48.
49. Stern, J. M.; Stanfield, J.; Kabbani, W.; Hsieh, J. T.; Cadeddu, J. A., Selective prostate cancer thermal ablation with laser activated gold nanoshells. *The Journal of urology* **2008,** *179* (2), 748-53.
50. Pardoll, D. M., The blockade of immune checkpoints in cancer immunotherapy. *Nat Rev Cancer* **2012,** *12* (4), 252-64.
51. Hodi, F. S., Cytotoxic T-lymphocyte-associated antigen-4. *Clin Cancer Res* **2007,** *13* (18 Pt 1), 5238-42.
52. Chakrabarti, L.; Morgan, C.; Sandler, A. D., Combination of Id2 Knockdown Whole Tumor Cells and Checkpoint Blockade: A Potent Vaccine Strategy in a Mouse Neuroblastoma Model. *PLoS One* **2015,** *10* (6), e0129237.
53. Postow, M. A.; Chesney, J.; Pavlick, A. C.; Robert, C.; Grossmann, K., et al., Nivolumab and ipilimumab versus ipilimumab in untreated melanoma. *N Engl J Med* **2015,** *372* (21), 2006-17.
54. Pilon-Thomas, S.; Li, W.; Briggs, J. J.; Djeu, J.; Mule, J. J.; Riker, A. I., Immunostimulatory effects of CpG-ODN upon dendritic cell-based immunotherapy in a murine melanoma model. *J Immunother* **2006,** *29* (4), 381-7.
55. Schwartzentruber, D. J.; Lawson, D. H.; Richards, J. M.; Conry, R. M.; Miller, D. M., et al., gp100 peptide vaccine and interleukin-2 in patients with advanced melanoma. *N Engl J Med* **2011,** *364* (22), 2119-27.
56. Chakrabarti, L.; Abou-Antoun, T.; Vukmanovic, S.; Sandler, A. D., Reversible adaptive plasticity: a mechanism for neuroblastoma cell heterogeneity and chemo-resistance. *Front Oncol* **2012,** *2*, 82.
57. Chakrabarti, L.; Wang, B. D.; Lee, N. H.; Sandler, A. D., A Mechanism Linking Id2-TGFbeta Crosstalk to Reversible Adaptive Plasticity in Neuroblastoma. *PLoS One* **2013,** *8* (12), e83521.
58. Cui, J.; Wang, N.; Zhao, H.; Jin, H.; Wang, G.; Niu, C.; Terunuma, H.; He, H.; Li, W., Combination of radiofrequency ablation and sequential cellular immunotherapy improves progression-free survival for patients with hepatocellular carcinoma. *Int J Cancer* **2014,** *134* (2), 342-51.
59. Fagnoni, F. F.; Zerbini, A.; Pelosi, G.; Missale, G., Combination of radiofrequency ablation and immunotherapy. *Front Biosci* **2008,** *13*, 369-81.
60. Maloney, E.; Hwang, J. H., Emerging HIFU applications in cancer therapy. *Int J Hyperthermia* **2015,** *31* (3), 302-9.
61. Sidana, A., Cancer immunotherapy using tumor cryoablation. *Immunotherapy* **2014,** *6* (1), 85-93.
62. Savoldo, B.; Rooney, C. M.; Di Stasi, A.; Abken, H.; Hombach, A., et al., Epstein Barr virus specific cytotoxic T lymphocytes expressing the anti-CD30zeta artificial chimeric T-cell receptor for immunotherapy of Hodgkin disease. *Blood* **2007,** *110* (7), 2620-30.

63. Durymanov, M. O.; Rosenkranz, A. A.; Sobolev, A. S., Current Approaches for Improving Intratumoral Accumulation and Distribution of Nanomedicines. *Theranostics* **2015,** *5* (9), 1007-20.
64. Meng, F.; Cheng, R.; Deng, C.; Zhong, Z., Intracellular drug release nano systems. *Materials Today* **2012,** *15*, 436-442.
65. Song, C., RobertPark, Heon Joo, Influence of Tumor pH in Therapeutic Response. In *Cancer Drug Discovery and Development: Cancer Drug Resistance*, Inc., B. T. H. P., Ed. Totowa, NJ, 2006; pp 21-42.
66. Fu, G.; Liu, W.; Feng, S.; Yue, X., Prussian blue nanoparticles operate as a new generation of photothermal ablation agents for cancer therapy. *Chem Commun* **2012,** *48*, 11567–11569.
67. Itaya, K.; Akahoshi, H.; Toshima, S., Electrochemistry of Prussian Blue Modified Electrodes: An Electrochemical Preparation Method. *J Electrochem Soc* **1982,** *129* (7), 1498-1500.
68. Karyakin, A. A., Prussian Blue and Its Analogues: Electrochemistry and Analytical Applications. *Electroanal* **2001,** *13* (10), 813-819.
69. Ribas, A., Anti-CTLA4 Antibody Clinical Trials in Melanoma. *Update Cancer Ther* **2007,** *2* (3), 133-139.
70. Langer, L. F.; Clay, T. M.; Morse, M. A., Update on anti-CTLA-4 antibodies in clinical trials. *Expert Opin Biol Ther* **2007,** *7* (8), 1245-56.
71. Ascierto, P. A.; Marincola, F. M.; Ribas, A., Anti-CTLA4 monoclonal antibodies: the past and the future in clinical application. *J Transl Med* **2011,** *9*, 196.
72. Callahan, M. K.; Postow, M. A.; Wolchok, J. D., Immunomodulatory therapy for melanoma: ipilimumab and beyond. *Clin Dermatol* **2013,** *31* (2), 191-9.
73. Snyder, A.; Makarov, V.; Merghoub, T.; Yuan, J.; Zaretsky, J. M., et al., Genetic basis for clinical response to CTLA-4 blockade in melanoma. *N Engl J Med* **2014,** *371* (23), 2189-99.
74. Schoenborn, J. R.; Wilson, C. B., Regulation of interferon-gamma during innate and adaptive immune responses. *Adv Immunol* **2007,** *96*, 41-101.
75. Zaidi, M. R.; Merlino, G., The two faces of interferon-γ in cancer. *Clin Cancer Res* **2011,** *17* (19), 6118-24.
76. Madhusudhan, A.; Reddy, G. B.; Venkatesham, M.; Veerabhadram, G.; Kumar, D. A.; Natarajan, S.; Yang, M. Y.; Hu, A.; Singh, S. S., Efficient pH dependent drug delivery to target cancer cells by gold nanoparticles capped with carboxymethyl chitosan. *Int J Mol Sci* **2014,** *15* (5), 8216-34.
77. Saboktakin, M. R.; Tabatabaie, R. M.; Maharramov, A.; Ramazanov, M. A., Synthesis and characterization of pH-dependent glycol chitosan and dextran sulfate nanoparticles for effective brain cancer treatment. *Int J Biol Macromol* **2011,** *49* (4), 747-51.
78. Kato, Y.; Ozawa, S.; Miyamoto, C.; Maehata, Y.; Suzuki, A.; Maeda, T.; Baba, Y., Acidic extracellular microenvironment and cancer. *Cancer Cell Int* **2013,** *13* (1), 89.
79. Cheng, L.; Gong, H.; Zhu, W.; Liu, J.; Wang, X.; Liu, G.; Liu, Z., PEGylated Prussian blue nanocubes as a theranostic agent for simultaneous cancer imaging and photothermal therapy. *Biomaterials* **2014,** *35* (37), 9844-52.
80. Dewhirst, M. F., JrRoemer RB, *Hyperthermia*. Gunderson LL, Tepper JE: New York, 2000.

81. Kapp, D., GMCarlson, RW, *Principles of Hyperthermia*. 5th Edition ed.; Hamilton, Ontario, 2000.
82. London, W. B.; Castel, V.; Monclair, T.; Ambros, P. F.; Pearson, A. D., et al., Clinical and biologic features predictive of survival after relapse of neuroblastoma: a report from the International Neuroblastoma Risk Group project. *J Clin Oncol* **2011,** *29* (24), 3286-92.
83. Boon, T.; Coulie, P. G.; Van den Eynde, B., Tumor antigens recognized by T cells. *Immunol Today* **1997,** *18* (6), 267-8.
84. Galon, J.; Costes, A.; Sanchez-Cabo, F.; Kirilovsky, A.; Mlecnik, B., et al., Type, density, and location of immune cells within human colorectal tumors predict clinical outcome. *Science* **2006,** *313* (5795), 1960-4.
85. Lee, S.; Margolin, K., Tumor-infiltrating lymphocytes in melanoma. *Curr Oncol Rep* **2012,** *14* (5), 468-74.
86. Zhang, L.; Conejo-Garcia, J. R.; Katsaros, D.; Gimotty, P. A.; Massobrio, M., et al., Intratumoral T cells, recurrence, and survival in epithelial ovarian cancer. *N Engl J Med* **2003,** *348* (3), 203-13.
87. Chew, A.; Salama, P.; Robbshaw, A.; Klopcic, B.; Zeps, N.; Platell, C.; Lawrance, I. C., SPARC, FOXP3, CD8 and CD45 correlation with disease recurrence and long-term disease-free survival in colorectal cancer. *PLoS One* **2011,** *6* (7), e22047.
88. Broere, F., Sergi GSitkovsky, Michail Vvan Eden, Willem, *T cell subsets and T cell-mediated immunity*. 3rd edition ed.; 2011.
89. de Souza, A. P.; Bonorino, C., Tumor immunosuppressive environment: effects on tumor-specific and nontumor antigen immune responses. *Expert Rev Anticancer Ther* **2009,** *9* (9), 1317-32.
90. Rabinovich, G. A.; Gabrilovich, D.; Sotomayor, E. M., Immunosuppressive strategies that are mediated by tumor cells. *Annu Rev Immunol* **2007,** *25*, 267-96.
91. Goldberg, M. S., Immunoengineering: how nanotechnology can enhance cancer immunotherapy. *Cell* **2015,** *161* (2), 201-4.
92. Pandian, V.; Ramraj, S.; Khan, F. H.; Azim, T.; Aravindan, N., Metastatic neuroblastoma cancer stem cells exhibit flexible plasticity and adaptive stemness signaling. *Stem Cell Res Ther* **2015,** *6* (1), 2.